AD-A079 592 BEN-GURION UNIV OF THE NEGEV BEERSHEBA (ISRAEL) F/G 20/12
DISLOCATION INFLUENCE ON THE ELECTRICAL AND OPTICAL PROPERTIES --ETC(U)
1979 S MIL'SHTEIN AFOSR-78-3526

UNCLASSIFIED AFOSR-TR-79-1355 NL

1 OF 2
AD A 079592

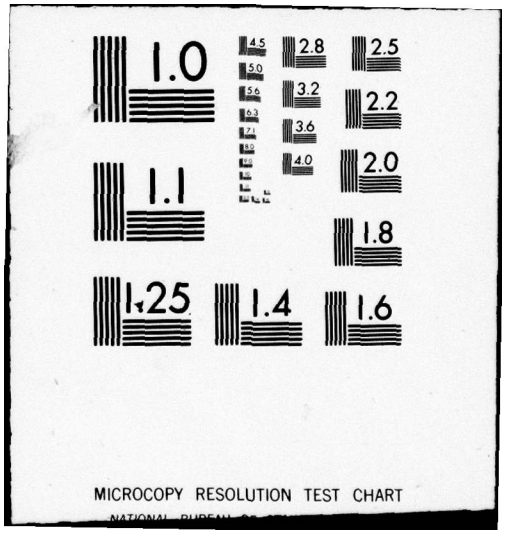
1.0
1.1
1.25
1.4
1.6
1.8
2.0
2.2
2.5
2.8
3.2
3.6
4.0
4.5
5.0
5.6
6.3
7.1
MICROCOPY RESOLUTION TEST CHART

(15) Contract/Grant Number: AFOSR-78-3526

(6) Dislocation Influence on the Electrical and Optical Properties of Semiconductors

391 189

(10) Samson Mil'shtein
Ben-Gurion University of the Negev
Beer-Sheva, Israel

(9) Final Scientific Report, 1 Jan [redacted]78 - 31 Mar [redacted]79

Approved for public release; distribution unlimited

(12) 104

(11) 1979

Prepared for:
Air Force Office of Scientific Research
Bolling AFB, D.C. 20332
and
European Office of Aerospace Research and Development
London
England

(18) AFOSR

(19) TR-79-1355



SIC 392 189

Contents

## Introduction

Investigation of dislocation influence on electrical and optical properties of both semiconductor materials and devices are currently in vogue [1-3]. If one knew the dislocation influence on electron state spectrum in semiconductors then most of the changes in properties of deformed semiconductors could be explained and even some predictions could be made. However, the concurrent presence of point defects (with their energy levels) [4] and Cottrell atmospheres complicates the problem and leads to ambigous information on the energy levels resulting from the presence of dislocations [5-6]. Part of the point defects could be thermally annealed in order to separate out the side effects. Therefore one of the main objects of the investigation was to separate outside effects, due to point defects, Cottrell impurity atmospheres, and the diffusion of gold during contact preparation, from the dislocation effects.

## Sample and contact preparation

Recently [7] we described the method of plastic deformation of

---


1. D. Gwinner, R. Labush, J. de Physique, 40, 6, 75 (1979).
2. U. del Penino, S. Mantovani, Phys. Stat. Solidi, A, 38, 109 (1967).
3. R. Labush, J. de Physique, 40, 6, 81 (1979).
4. J. Corbett, Phys. Rev. B, 5, 2337 (1978).
5. R. Jones, J. de Physique, 40, 6, 33 (1979).
6. R. Labush, R. Schettler, Phys. Stat. Solidi, A, 9, 455 (1972).
7. S. Mil'shtein, J. Appl. Phys. 46, 9, 3894 (1975).

the specimens and their thermal annealing. We also developed a new method of $CO_2$ laser shocking, which creates a high dislocation density clusters in semiconductor crystals. This method was developed in order to avoid a possible contamination of the bulk of crystal by impurities, which could easily diffuse into the crystal under high temperature and pressure conditions during plastic deformation.

Using short (0.1 sec). pulses of $CO_2$ irradiation with energy of about 60 joul we shocked the silicon (intrinsic conductivity) plates. Investigating the dislocation structure in those samples we find a high density of edge type dislocations [$10^{10}$-$10^{11}$ $cm^{-2}$].

The same chemical treatment [7] was given to both plastically deformed and thermally shocked specimens.

The ohmic contacts were welded [8] to the dislocation-free and deformed parts of the crystals by condenser welding. The welding is advantageously affected in such a manner that local overheating and diffusion of the contact materials are avoided.

Measurements and evaluations

Characterization of the dislocated specimens were served by high voltage transient electron microscopy (TEM) and by metallographic methods as well [9]. The specimens for TEM investigation were thinned to a thickness of about 1-2 μk. The microscope used the power up to

---

8. S. Mil'shtein, U.S.A. patent 611801 from 9.9.1975.

9. M. Brown and A. Willoughby, J. de Physique, 40, 6, 151 (1979).

1.2 Mev [10].

. Electrical measurements include the photoconductivity measurements [11] (see appendix, A and B) and the investigation on C-V characteristics of dislocation p-n junction (see appendix F).

The differential photoconductivity measurements completely described in appendix B. The capacity measurements were performed on thin (200 μK) Si speciments (5 × 5 $mm^2$) by the aid of Automatic Capacitance Bridge (Model 4270A, Hewlett-Packard) at room temperatures [12].

Theoretical evaluation of electrical barriers due to single dislocations (SDEB) in Si and Ge in wide temperature range was performed (see appendix D). The possibility to measure the internal Frantz-Keldysh effect in the vicinity to single 60° dislocation in Si and Ge is also considered.

It was developed and experimentally tested the new method of photoconductivity measurements for both, the case of the photoconductivity near fundamental absorption edge (see appendix B) and for photoconductivity generated from deep states (impurities, point defects and dislocations) as well (see appendix G)

---

[10] H. Föll and B. Kollesen, J. Appl. Phys. 8 319 (1975).
[11] S. Mil'shtein and A. Senderichin, Israeli Phys. Soc. 25, 20 (1979).
[12] S. Mil'shtein, J. de Physique 40, 6, 207 (1979).

## Results

The only results, which are neither published nor submitted for publication are presented in the main part of the current report. The rest of the results can be found in appendices A-G.

Using $CO_2$ powerful laser we shocked Si specimens. Investigation of damaged area by TEM shows that the area contains edge dislocations of high density ($10^9$ - $10^{10}$ $cm^{-2}$). Figure 1, shows the central part of clusters with edge type dislocations with Burger's vector < 220 > . Magnification of the picture 1 is of about 10000 times. Figure 1b, shows the peripheral part of dislocation cluster. One can see, that most of the dislocations have edge components the density reduced by factor 20 comparatively to the central part of the cluster, (see Fig. 1a).

The [111] surface was irradiated by 0,1 sec. pulses. Shortening of the pulse proportionaly results in decreasing of dislocation density. But pulses longer than 0,1 sec had destroyed the specimens.

Let us explain the mechanism of thermal laser shock. From the very beginning the Si or Ge wafer absorbs small parts of J.R. radiation. But absorption coefficients of the material increases exponentionaly with increasing temperature of the sample. This process takes time and then 80% of radiation is absorbed. So the melting-recrystallization process itself is very short. The TEM and x-ray examinations show that the specimen becomes monocrystal after all. Epitaxial regrowing process seems to be a reasonable explanation of this fact.

The dislocation diode effect was observed at dislocation clusters after laser irradiation . In accordance with our programme the photo conductivity measurements were carried out on dislocated Si (see Appendix B). The specimens were cut in the form of a bar with the dimensions 0.5 × 3 × 40 mm. The [111] surface were illuminated by the Halogen lamp. The Ir-20 monochromator (Joubin Yovin) was used. Figure 2 presents the photoconductivity of controled specimen near the fundamental absorption edge. The energy gap can be easily determined by the slope of the curve.

Figure 3 shows the photoconductivity of plastically deformed Si n-type. One can see the additional peak of photoconductivity due to wave length of about 0,7 μK. Being repeated our measurement shows the same result on laser irradiated specimens. No shift of observed peaks occurred under liquid nitrogen temperature.

Measuring the capacity C of dislocation p-n junction at frequency of 10 Khz. and 1 Mhz. we found that C is in a limit from 20 pf. to 80 pf. approximately. The value of C is straightly connected to conditions (loading temperature and time) of plastic deformation process.

Discussion

Let us discuss first the theoretical results we got:

1. In accordance with the 1st paragraph of the programme we calculated the electrical barrier due to single dislocation (SDEB) in Si and Ge. This work (see appendix D) is now in press. The important results, from our

point of view, are the following:

a) We proposed the new model of single edge type dislocation in tetraedraly coordinated semiconductors. It was found by us that neither DC nor microwave conductivity along the dislocation "core" is likely to exist. It appears that electrical model of a single edge-type dislocation described in the literature behaving like cylindrical p-n structure able to work like delay line [13] is not quite correct. According to our model, carriers are spreading out of the dislocation i-type cylinder, are crossing i-n interface, where the rectification take place. In terms of equivalent scheme there is a half loop of two i-n diodes connected in opposite to each other. The possible application of such a scheme in monalitic circuits is discussed [12] (see appendix C).

b) The general solution for the problem of finding the electrical potential distribution around a single charged dislocation line is obtained. In the wide temperature range SDEB dependence on type of dislocation, concentration of impurities is computed. We hope our results would serve as handbook data.

2. In accordance with the 3rd paragraph of the programme we investigated the possibility of experimental observation of the internal Franz-Keldysh Effect at single dislocation in Si and Ge. Our calculation shows that this effect might be expected in Si with donor concentration $N_d$ up to $10^{16}cm^{-3}$ and in Ge with $N_d$ up to $10^{15}cm^{-3}$ in wide temperature

---

13. W. Bardsley, in book "Progress in Semiconductors", Wiley, N.Y. 1960 v.4, p.157.

range from 100 K up to 400 K. The experimental details are discussed (see appendix G).

Let us discuss now the experimental results.

3. In accordance with paragraph 2 of the programme we investigated the electron state spectrum of dislocated semiconductors by the aid of dislocation diode effect (see appendix F). Our measurements show the existence of dislocation acceptor $E_a$ = 0.39 ev in laser irradiated Si and in mechanically deformed Si as well. The model of the dislocation p-n junction is used to determine the width of the dislocation energy band, which apparently does not exceed several hundreths of electronvolt. This new important result contradicts data published recently [14, 15]. The electric neutrality equation has been used to analyse the dislocation electrical barrier (DEB) and the conditions of its existance in Si and Ge in wide temperature range.

We found that the dislocation diode effect is to be expected even in the materials with low resistivity, up to $10^{16} cm^{-3}$.

4. In order to describe the role played by dislocations, we carried out the characterization of dislocation structures by TEM. The TEM examination shows that "pure" dislocation structures are created by laser irradiation. Figures 1a and 1b demonstrate the edge type dislocations of high density. True, such irradiation might evoke segregation of impurities in a crystal

---

14. R. Jones, Phil. Mag. 36, 3, 677 (1977).

15. D. Mergel, R. Labusch., Phys. Status. Solidi 42, 165 (1977).

and might result in Cottrell atmospheres formation but the melting-recrystallization process is itself so short that there is no time for diffusion of impurities from outside. Laser irradiation makes it able to avoid the general heat treatment of specimens which is necessary for any of mechanical plastic deformation methods. However, we did not answer yet many questions due to the role of point defect and impurity clouds, if any, in the crystals irradiated by $CO_2$ laser. And, in our opinion, this investigation must be continued.

5) The C-V measurements [16,17] are the base of transient capacitance spectroscopy, which is among the main methods being used for investigation on defect induced energy states.

In accordance with paragraph 2 of the programme we developed a C-V measurements [12] (see appendix C) of dislocation p-n junction which can be obtained "abrupt" under certain conditions of plastic deformation process. Measuring $1/C^2$ versus reverse bias voltage we found for Si with $N_d = 10^{14}cm^{-3}$ the density of dislocation, acceptors of about $2 \times 10^{15}cm^{-3}$ and that is equivalent to the dislocation density $N_{disl} \approx 1{,}3 \cdot 10^{9}cm^{-2}$. Control measurements by the aid of the electron microscope revealed $N_{disl}$ of about $8.6 \cdot 10^{8}cm^{-2}$, which agrees well with C-V measurements. Therefore, capacitance measurements furnish a simple way of determining the density of acceptors in a deformed part of the crystal, i.e. the dislocation density.

Calculating the net charge concentration in the depletion area

---

16. S. Mantovani, U. del Penino and E. Mazega, Phys. Stat. Solidi A, 35, 451 (1976).

17. J. Patel and C. Kimerling, J. de Physique, 40, 6, 101 (1979).

one can easily find the position of Fermi level which is usually pinned to the middle of dislocation band. In other words, obtaining the Fermi level $(E_v + 0.37)$ev, we determined the position of dislocation acceptors.

Unfortunately, the originally small value of capacity of the dislocation p-n junction becomes comparable to the "parasite" capacities of our crogenic equipment, the fact which had distorted the low temperature measurements.

We are dealing with the interface between dislocated part of crystal and nondeformed one instead of the Schottky barrier. In our opinion these measurements being made on dislocation p-n junctions has certain advantages in comparison to the same measurements on Schottky diodes with their complicated contact problems.

6. In accordance with paragraph 4 of the programme we carried out the photoconductivity measurements on n-type silicon in order to obtain the information about the energy states due to dislocations. There is an additional photoconductivity peak near the fundamental absorption edge on a wave length of about 0.7 μk, which is equivalent to photon energy of about 1.76 ev. This strange result was repeatedly obtained on a number of plastically deformed and laser shocked specimens and can be attributed to changes in the shape of the conduction band.

7. In addition to our programme we developed and tested a new method [11](see appendicies A,B, and G) of photoconductivity measurements which

enable us to eliminate from the consideration a surface influence. It is proposed to measure transversal photoconductivity in three layers, what supplies the investigator by some optical constants like absorption coefficients, quantum yield, diffusion length etc. This method can be used for intrinsic doped semiconductors and those contain deep centers like dislocations and point defects as well (see appendix G).

Comments

The results of the investigations carried out under U.S. Air Force support in the period from 1.1.78 to 1.3.79 were presented at two conferences:

1. Annual Meeting of the Israeli Physical Society which was held in Beer-Sheva, Israel. The abstracts were published (see Appendix A).
2. International Symposium on Dislocations in Tetraedrally Coordinated Semiconductors, which was held in Hünfeld, West Germany.

   The proceedings were published (see Appendix C).

In addition to the above mentioned publications we submitted another five manuscripts, which are now in press.

We are planning to submit in the near future two manuscripts entitled:

1. "Dislocation energy states in Si defined by C-V measurements" by S. Mil'shtein.
2. "Photoconductivity of heavily dislocated Si" by S. Mil'shtein.

These two pieces of work are certainly supported by the current

grant from U.S. Air Force, but the results are not ready to be published at this very moment.

To demonstrate our achievements in the discussion we would like to point out the shortcomings of our research due to spectral sensitivity of the dislocation p-n junction, which we did not measure. Ths reason for this is some geometrical problems troubling the use of the dislocation p-n junctions like photocells. True, these problems are not solved until this very moment.

It must be pointed out that the current program was "overloaded" i.e. we tried to do more than possible for the 15 months programme. This is certainly a result of the proposal presented by the principal investigator. On the other hand, trying to publish the main results we delayed the final report which is again the fault of the principal investigator.

References


1. D. Gwinner, R. Labush, J. de Physique, 40, 6, 75 (1979).
2. U. del Penino, S. Mantovani, Phys. Stat. Solidi, A, 38, 109 (1967).
3. R. Labush, J. de Physique, 40, 6, 81 (1979).
4. J. Corbett, Phys. Rev. B, 5, 2337 (1978).
5. R. Jones, J.de Physique, 40, 6, 33 (1979).
6. R. Labush, R. Shettler, Phys. Stat. Solidi, A, 455 (1972).
7. S. Mil'shtein, J. Appl. Phys. 46, 9, 3894 (1975).
8. S. Mil'shtein, U.S.A. patent 611801 from 9.9.1975.
9. M. Brown and A. Willoughby, J. de Physique, 40, 6, 151 (1979).
10. H. Foll and B. Kollesen, J. Appl. Phys. 8, 319 (1975).
11. S. Mil'shtein and A. Senderichin, Israeli Phys. Soc. 25, 20 (1979).
12. S. Mil'shtein, J. de Physique 40, 6, 207 (1979).
13. W. Bardsley, in book "Progress in Semiconductors", Wiley, N.Y. 1960 v.4, p.157.
14. R. Jones, Phil. Mag. 36, 3, 677 (1977).
15. D. Mergel, R. Labush, Phys. Status. Solidi, 42, 165 (1977).
16. S. Mantovani, U. del Penino and E. Mazega, Phys. Stat. Solidi A, 35, 451 (1976).
17. J. Patel and C. Kimerling, J. de Physique, 40, 6, 101 (1979).

Captions

Fig.1. TEM examination of laser irradiated Si.

a) Central part of dislocation cluster.

b) Peripherial part of dislocation cluster.

Fig.2. Photoconductivity of non-deformed n-type Silicon.

Fig.3. Photoconductivity of dislocated n-type Silicon.

Fig.1. TEM examination of layer irradiated Si.

a) Central part of dislocation cluster

b) Peripherial part of dislocation cluster.

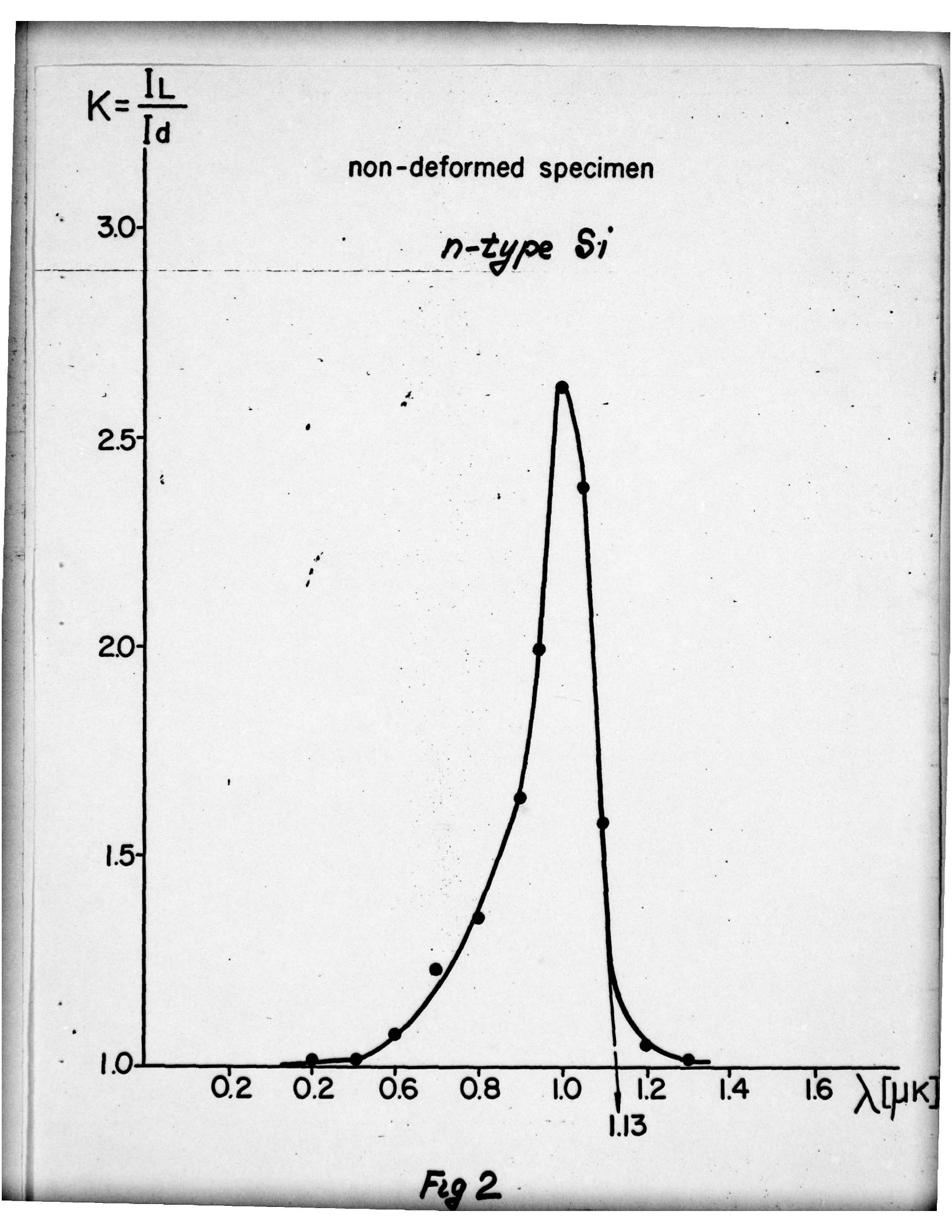
K = IL / Id
non-deformed specimen
n-type Si
3.0
2.5
2.0
1.5
1.0
0.2
0.2
0.6
0.8
1.0
1.13
1.2
1.4
1.6
λ [μK]

Fig 2

$K = \frac{I_K}{I_d}$

Fig 3

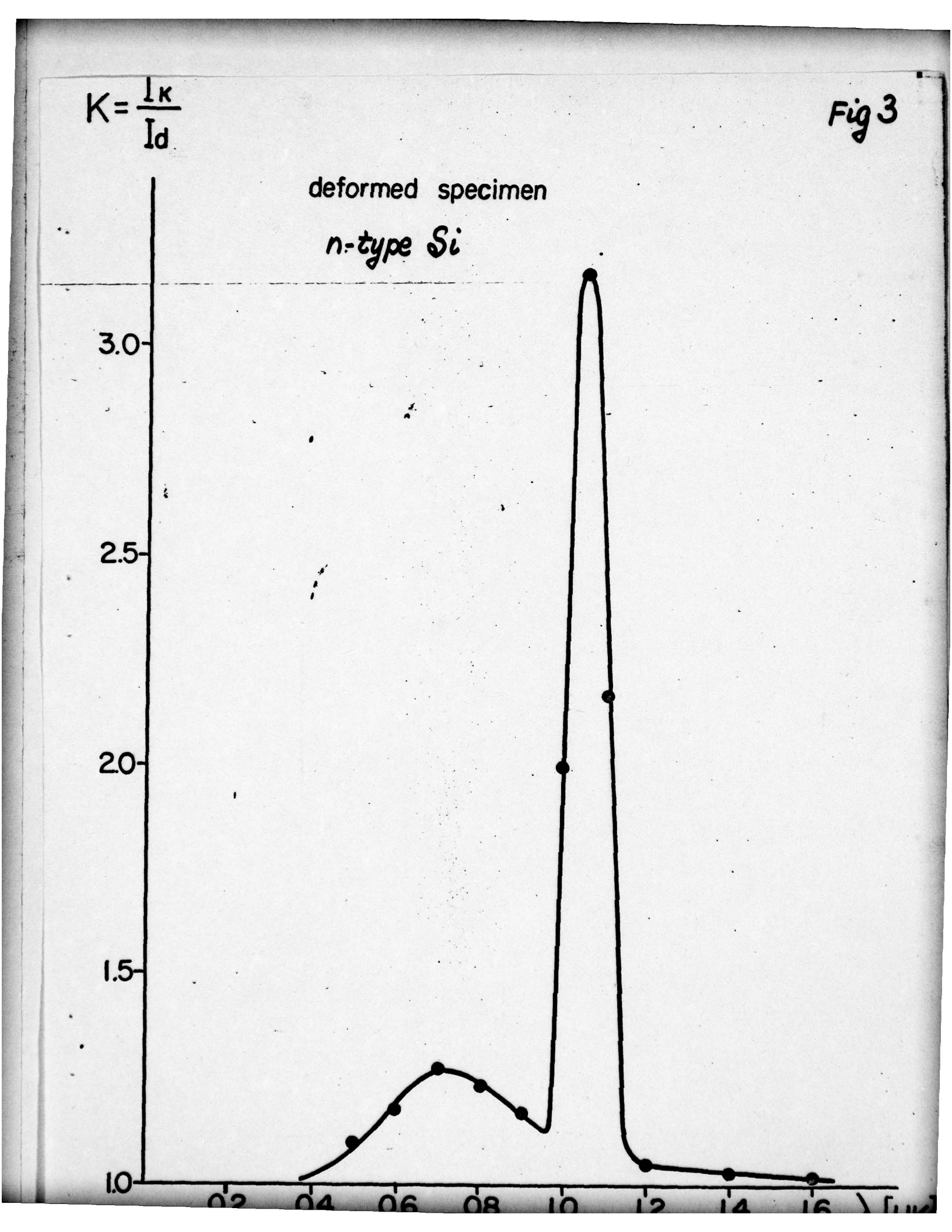

Appendix A

# BULLETIN OF THE ISRAEL PHYSICAL SOCIETY

v 25, 1979

1979
Annual Meeting
PROGRAM
and
ABSTRACTS

SUNDAY AFTERNOON, 1 APRIL 1979
14:30

LIBRARY BUILDING
(Room 326)

C. APPLIED PHYSICS
K. Weiser, Israel Institute of Technology, Haifa - Presiding

C-1

## New Method of Photoconductivity Measurement*

G. Mil'shtein and A. Senderichin
Department of Physics, Ben Gurion University of the Negev
Beer Sheva, Israel

The spectral dependence of photoconductivity might give detailed information about the energy gap and the impurity levels within the gap only in the case when the spectral dependence of the absorption coefficients $\alpha(\lambda)$ is known. Determination of $\alpha(\lambda)$ from reflectivity and transparency measurements is limited by the accuracy of finding $I_0 = I(1-R)$, which strongly depends on surface state, since $R$ is the reflectivity coefficient.[1] The excess photocondictivity $\Delta\sigma$ also depends on surface parameters as surface recombination velocity s.[2] Trying to avoid the difficulties mentioned above we developed a new method of photoconductivity measurements. Taking into account the bulk generation-recombination processes and the surface recombination as well, the excess photoconductivity can be presented

$$\Delta\sigma = \beta(\mu_n\tau_n + \mu_p\tau_p)eI_0 \cdot (1-e^{-\alpha x}) - \mu_s e \Delta n_s(L_d,s) \qquad (1)$$

where $\beta$ is the quantum efficiency, $\mu_s$ - the surface mobility,

$\Delta n_s(L_d,s)$ - excess concentration on the surface as a function of the diffusion length and the surface recombination velocity.

Measuring the transversal photoconductivity $\Delta\sigma(x)$ for three layers lying on different depths we obtain:

$$\frac{\Delta\sigma(x_2) - \Delta\sigma(x_1)}{\Delta\sigma(x_3) - \Delta\sigma(x_1)} = \frac{e^{-\alpha x_2} - e^{-\alpha x_1}}{e^{-\alpha x_3} - e^{-\alpha x_1}} \qquad (2)$$

Equation (2) enables us to calculate the absolute value of $\alpha(\lambda)$ from the measured values of the photoconductivities $\Delta\sigma_1$, $\Delta\sigma_2$, $\Delta\sigma_3$. The derived spectral distribution of $\alpha$ facilitates solving the problem of finding the other parameters of the material.

* Supported by US Air Force under grant AFOSR-78-3526.

1. J. Pankove, "Optical processes in semiconductors", (1971).

2. T.S. Moss and T.D.H. Hawkins, Phys. Rev. Letters, Vol. 1, No. 4, 129-130 (1958).

# Appendix B

## Determination of Optical Constants Near the Fundamental Absorption Edge in Semiconductors*

S. Mil'shtein, A. Senderichin

Department of Physics, Faculty of Natural Sciences,
Ben-Gurion University of the Negev, Beer Sheva, Israel

**Abstract**

The photoconductivity of semiconductors is considered under general conditions: the surface recombination velocity s not equal to zero, the space charge near the surface exists , the value of absorption coefficient $\alpha$ is not limited. Solving both the continuity and Poisson equations for illuminated thick specimen, we obtained the solution which suggests a new combined measurement in order to determine various optical constants. Experimental details are discussed.

Submitted to Phys. Rev.

* Supported by U.S. Air Force

## Introduction

Fundamental absorption caused by the electron band to band transitions in the range of wave lengths from 0.12μm to 1.5μm can be observed in semiconductors [1]. In order to investigate the fundamental absorption edge one can measure the transparency of a crystal [2] or its reflectivity [3] that is analyzed by means of Kramers-Kronig's relations [4]. The information on the absorption can be obtained from photoconductivity measurements as well. Moss and Hawkins measured photoconductivity for thick specimens [5] but in their work there are principle errors which we will discuss later. While the thickness of a crystal is of no importance in the case of the reflectivity measurement, in the case of the transparency measurement thin crystals are generally used, particularly when exciton absorption is being considered. Unlike these two methods, the photoconductivity measurements may be carried out for any thickness therewith, obtaining a various information: in the case of thick samples the photo-response is determined by life time and mobility of carriers, while in the case of thin samples it depends on the intensity of absorbed light.

For the above mentioned experimental methods there is a general difficulty connected with the fact that for any optical measurement incident light intensity $I_0$, and intensity of reflected light should be known. Otherwise the reflectivity coefficient R and intensity of transparated light $I = I_0(1-R)$ should be known. These values are linked strongly to the quality of surface treatment. The problem is more complicated by the necessity of creating identical conditions on a surface of two samples: the tested and the controlled. Analysis of photoconductivity and of

fundamental absorption mechanisms is based on the solution of continuity and of Poisson's equations with space electrical charge near the surface. Unfortunately these equations are solved by simplified assumptions as for example the absence of surface recombination (s=0) and by neglecting space charge near the surface ($\rho \approx 0$) or under the assumption of a small absorption coefficient ($\alpha < 1$) [6].
In the present work we have solved the above mentioned equations in a most general case. The new experimental method of photoconductivy measurements is suggested.

## Theory

Let us consider an infinite semiconductor specimen in the form of a rectangular prism illuminated by light from one side. The light intensity is $I\left(\frac{1}{cm^2 sec}\right)$ and surface recombination velocity is s (cm/séc.). As a result of electron-hole pairs generation by light the diffusion and drift of excess carriers $\Delta n$, $\Delta p$ occur in the crystal. These drift and diffusion currents can be expressed:

$$J_p = - e D_p \frac{d\Delta p}{dx} + e \mu_p pE \qquad (1)$$

$$J_n = e D_n \frac{d\Delta n}{dx} + e \mu_n nE \qquad (2)$$

In the static case the total current is zero:

$$J_p + J_n = 0 \qquad (3)$$

The continuity equation can be written in the form:

$$\frac{dJ_p}{dx} = e\beta\alpha\, I \exp(-\alpha x) - \frac{e(p\Delta n + n\Delta p)}{(p+n)\tau} \qquad (4)$$

where $\alpha$ is absorption coefficient

$\beta$ is quantum yield.

$x$ is the current coordinate in the direction of light propagation

All other designations, used in the equations (1-4) are generally accepted.

For simplicity we will use below the designations:

$$b = \frac{\mu_n}{\mu_p} \; ; \qquad \frac{J_p}{e} = J \; .$$

The excess carriers $\Delta n$ and $\Delta p$ generated near the surface may give rise to a space electric charge, that by means of Poisson's equation is described:

$$\frac{dE}{dx} = \frac{e}{\varepsilon\varepsilon} [\Delta p - \Delta n] \qquad (5)$$

Combining the equations (1)-(4) we obtain:

$$\frac{d^2J}{dx^2} - \frac{J}{L^2} = -\beta\alpha^2\, I \exp(-\alpha x) \qquad (6)$$

where

$$L^2 = D_p \tau \frac{p+n}{\frac{p}{b} + n}$$

is the diffusion length of ambipolar diffusion.

The differential equation (6) is solved under the boundary conditions

$$J(0) = - s \cdot \Delta p(0) \tag{7}$$

$$J(\infty) = 0 . \tag{8}$$

As far as $\Delta p(0)$ is unknown the solution of equation (6) will contain an unknown integration constant B:

$$J = B \exp\left(-\frac{x}{L}\right) - I\,\alpha^2\beta \cdot \exp(-\alpha x)\,\frac{1}{\alpha^2 - L^{-2}} \tag{9}$$

Solving the system of equations (1), (2), (5) and using the formula (9) we obtain the equation for the electric strength E:

$$\frac{d^2E}{dx^2} - \frac{1}{d^2}E = - \frac{(b-1)e}{bD_p \varepsilon\varepsilon_0}\left[Be^{-x/L} - I\alpha^2\beta \exp(-\alpha x)\,\frac{1}{\alpha^2 - L^{-2}}\right] \tag{10}$$

where

$$d = \sqrt{\frac{D_p \varepsilon\varepsilon_0}{e\mu_p (p+n)}} \tag{10a}$$

is the distance of Maxwell relaxation.

The equation (10) is solved under the boundary conditions:

$$E(0) = 0 \tag{11}$$

$$E(\infty) = 0 \tag{12}$$

that express an electrical neutrality of the sample in general.

The solution of equation (10) is:

$$E = \left(\frac{b-1}{b}\right) \frac{1}{\mu_p} \frac{1}{(p+n)} \left[\frac{I\alpha^2\beta}{(\alpha^2-L^{-2})(1-\alpha^2d^2)} \left(e^{-x/d} - e^{-\alpha x}\right) - \right.$$

$$\left. - \frac{B}{1-\frac{d^2}{L^2}} \left(e^{-x/d} - e^{-x/L}\right)\right] \qquad (13)$$

where constant B is still unknown.

From equation (1) we define the expression $\frac{d\Delta p}{dx}$, determined by J - current and E - electric strength in accordance with (9) and (13). Performing the integration under the conditions $\Delta p = 0$ when $x \to \infty$ we obtain the dependence $\Delta p(x,B)$. Using the expression (9) we can find the constant B from the condition (7). Finding the value B and substituting it into $\Delta p(x,B)$ we obtained the final expression $\Delta p(x)$:

$$\Delta p(x) = I\left\{\left[B^* \frac{1}{1-\frac{d^2}{L^2}} - \frac{\alpha^2\beta}{(\alpha^2-L^{-2})(1-\alpha^2d^2)}\right] \cdot \left(\frac{b-1}{b}\right) \left(\frac{p}{p+n}\right) \frac{d}{D_p} e^{-x/d} + \right.$$

$$+ B^* \frac{L}{D_p} \left[1 - \frac{1}{1-\frac{d^2}{L^2}} \left(\frac{b-1}{b}\right) \left(\frac{p}{p+n}\right)\right] e^{-x/L} -$$

$$\left. - \frac{1}{D_p} \frac{\alpha\beta}{\alpha^2-L^{-2}} \left[1 - \frac{1}{1-\alpha^2d^2} \left(\frac{b-1}{b}\right) \left(\frac{p}{p+n}\right)\right] e^{-\alpha x}\right\} \qquad (14)$$

where for the sake of simplicity we designate:

$$B^*(\alpha,\beta,L,s,d,D_p) \equiv \frac{\frac{\alpha\beta}{\alpha^2-L^{-2}}\left(\alpha+\frac{s}{D_p}\right)-\frac{s}{D_p}\left(\frac{b-1}{b}\right)\left(\frac{p}{p+n}\right)\frac{\alpha^2\beta}{\alpha^2-L^{-2}}\cdot\frac{1}{1+\alpha d}}{1+\frac{sL}{D_p}-\frac{sL^2}{L+d}\cdot\frac{1}{D_p}\left(\frac{b-1}{b}\right)\cdot\left(\frac{p}{p+n}\right)} \tag{15}$$

Further it is easy to obtain an expression for $\Delta n(x)$

$$\Delta n(x) \equiv I\left[B^*\frac{1}{1-\frac{d^2}{L^2}}-\frac{\alpha^2\beta}{(\alpha^2-L^{-2})(1-\alpha^2d^2)}-\frac{p+n}{p}\right]\cdot\left(\frac{b-1}{b}\right)\cdot\left(\frac{p}{p+n}\right)\frac{d}{D_p}e^{-x/d}+$$

$$+B^*\frac{L}{D_p}\left[1-\frac{1}{1-\frac{d^2}{L^2}}\left(\frac{b-1}{b}\right)\left(\frac{p}{p+n}\right)+\left(\frac{b-1}{b}\right)\frac{d^2}{L^2}\frac{1}{1-\frac{d^2}{L^2}}\right]e^{-x/L}-$$

$$-\frac{1}{D_p}\frac{\alpha\beta}{\alpha^2-L^{-2}}\left[1-\frac{1}{1-\alpha^2d^2}\left(\frac{b-1}{b}\right)\left(\frac{p}{p+n}\right)+\frac{\alpha^2d^2}{1-\alpha^2d^2}\left(\frac{b-1}{b}\right)\right]e^{-\alpha x} \tag{16}$$

The equations (16), (14) for excess electrons $\Delta n(x)$ and for excess holes $\Delta p(x)$ contain three terms with exponential dependence $\exp(-\frac{x}{d})$; $\exp(-\frac{x}{L})$; $\exp(-\alpha x)$.

## Results

If one knows the distribution of excess concentration $\Delta n(x)$ and $\Delta p(x)$ are the excess photoconductivity in layers which/perpendicular to the direction of light can be found. The following two cases are of particular interest:

a) High-resistance semiconductors

In high-resistance semiconductors there is a Dember effect, determined by means of the factor $\exp(-x/d)$ in equations (14), (16). For the photoconductivity measurements in a layer close to the surface one must use the full expressions (14), (16) for $\Delta n(x)$; $\Delta p(x)$, that contain three terms, and the parameter $d$ that needs to be measured in any manner. Obviously, in the layers far from the surface, i.e., if $x \gg d$ there is no necessity to take into account the first term in equations with $d$, since $\exp(-x/d) \to 0$. In Fig. 1 the computation of Maxwell relaxation distance $d$ as a function of free carrier concentration and of temperature in Si is presented. The same dependence of $d$ for Ge is given in Fig. 2. As seen from Figures 1, 2 the value of $d$ sharply decreases with an increasing in concentration and temperature. For Si with concentration $10^{13}$ cm$^{-3}$ $d$ reaches fractions of a micron. Even for very high-resistance semiconductors with concentration $\approx 10^{10}$ cm$^{-3}$ for Si and $10^{13}$ cm$^{-3}$ for Ge. $d$ will be of order $10^{-3}$ cm at room temperature! Consequently choosing $x$ equal to $10^{-2}$ cm, i.e., measuring photoconductivity in the layer situated at the distance $10^{-2}$ cm from the surface we may neglect the Dember effect, and the first terms of the equations (14,16) may be omitted.

b) Low-resistance semiconductors

In low-resistance semiconductors with high concentration of free carriers the Dember effect does not appear, and the equations contain only the second and the third terms. The proposed method of measurement

will be more exact if the current would not spread out from the considered layers. Obviously this condition is correct when the width of electrodes is greater than the distance between them. As shown in Fig. 3 the specimen must be a narrow bar (a×b×c). To decrease the spreading effect a pair of very narrow guard electrodes on the left and on the right side from the basic electrodes are attached. It is sufficient to set these two guard electrodes on one side of the specimen. In the case of guard electrodes the dark currents $i_1$, $i_2$, $i_3$ were measured for each of the three layers. Then the current measurement was performed when these layers were connected in parallel. We found that the law of current superposition is fulfilled. Measuring photoconductivity three times for three layers situated at different depths, we can use a system of two non-linear equations for two unknown quantities $\alpha$ and $L$:

$$\frac{G_1 e^{-x_2/L} - G_2 e^{-x_1/L}}{G_1 e^{-x_3/L} - G_3 e^{-x_1/L}} = \frac{e^{-\alpha x_1} \cdot e^{-x_2/L} - e^{-\alpha x_2} \cdot e^{-x_1/L}}{e^{-\alpha x_1} \cdot e^{-x_3/L} - e^{-\alpha x_3} \cdot e^{-x_1/L}} \qquad (17)$$

$$\frac{G_1 e^{-x_2/L} - G_2 e^{-x_1/L}}{G_2 e^{-x_3/L} - G_3 e^{-x_2/L}} = \frac{e^{-\alpha x_1} e^{-x_2/L} - e^{-\alpha x_2} e^{-x_1/L}}{e^{-\alpha x_2} e^{-x_3/L} - e^{-\alpha x_3} e^{-x_2/L}}$$

The quantities $G_1$; $G_2$; $G_3$; $x_1$; $x_2$; $x_3$ are measured in the experiment.

Discussion

1. In the proposed method the relative measurements of photoconductivity enable us to eliminate from the consideration a surface influence and the necessity to measure, in particular, the intensity of reflected light. This is essential when producing a smooth and clean surface is very difficult.

2. It is possible to exclude also the available space charge near the surface (Dember effect) in high-resistance semiconductors by measure photoconductivity in the layers situated far away from the surface, so the distance $x$ larger than $d$- the Maxwell relaxation length.

3. It is proposed to measure a transversal conductivity in the selected layers, i.e., the conductivity when the electric field is perpendicular to the incident light. Our measurements have shown that only in the case with guard electrodes no current spreading occurs. Therefore the values $G_1$; $G_2$; $G_3$ can be measured quite correctly.

Moss and Hawkins [5] measured the longitudinal conductivity when the electric field was applied along the thick specimen and light propagation vector was parallel to the vector of the electric field. Assuming that photosensitivity is proportional to the number of absorbed photons, Moss carried out an integration

$$S = \frac{\Delta G}{I} = C\alpha \int_{x_1}^{x_2} \exp(-\alpha x)\,dx = C(e^{-\alpha x_1} - e^{-\alpha x_2}) \qquad (18)$$

where $C$ - coefficient of proportionality.

In fact, the integral in the expression (18) means the summation over conductivities in the specimens with a nonuniform distribution of excess carriers. But one can easily see that integration of the resistances of elementary layers and not their conductivities was performed. In regard to the presented results [5] it is difficult to understand how the expression (18) for photoconductivity could be obtained. Obviously, providing the small quantity of excess carriers, i.e., $\Delta n << n$ equations similar to the equations (18) given by Moss for thick samples can be obtained [ 6 ]. But it means the experiment with very low intensity of illumination and the small photoresponse, respectively.

4. System of equations (17) enables us to obtain from the relative value of photoconductivity the absolute value $\alpha$, i.e., the spectral dependence of the absorption coefficient $\alpha$. Without much trouble we can obtain from that system the diffusion length, that is an important parameter of material. Subsequently, the equations (17) enable us to obtain quantum yield $\beta$ and other constants of material. In the literature [ 6 ] the expressions for excess concentrations were obtained by simplified assumptions $\alpha << 1$. That means the mathematical description is valid only for the optical range where materials have a small $\alpha$. In our case the system of the equations is correct for any value $\alpha$.

The disadvantage of the proposed method is the necessity to use thick specimens. Therefore we cannot use this method for example in an exciton absorption range.

The authors gratefully acknowledge the support of the Air Force Office of Scientific Research and EOARD who sponsored this work under grant AFOS-78-3526.

## References

[1] T. McLean, Progr. Semicond., 5, 55 (1960).

[2] M. Cardona and G. Harbeke, Journ. Appl. Phys. 34, 813 (1963).

[3] H. Philipp, W. Dash and H. Ehrenreich, Phys. Rev. 127, 762 (1962).

[4] T. Robinson, Proc. Phys. Soc. B65, 910 (1952).

[5] T. Moss and T. Hawkins, Phys. Lett. 1, 129 (1958).

[6] T. Moss, G. Burrell and B. Ellis, in book "Semiconductor Opto-Electronics", Butterworth and Co., 1973, p. 103.

## Figure Captions

Fig. 1. Maxwell relaxation distance d versus donor concentration in Si for various temperatures:

1) -200°C, 2) -100°C, 3) 0°C, 4) +100°C, 5) +200°C

Fig. 2. Maxwell relaxation distance d versus donor concentration in Ge for various temperatures:

1) -200°C, 2) -100°C, 3) 0°C, 4) +100°C, 5) +200°C

Fig. 3. Sketch of specimen for the transversal photoconductivity measurements:

m - main electrodes; g - guard electrodes.

Fig 1

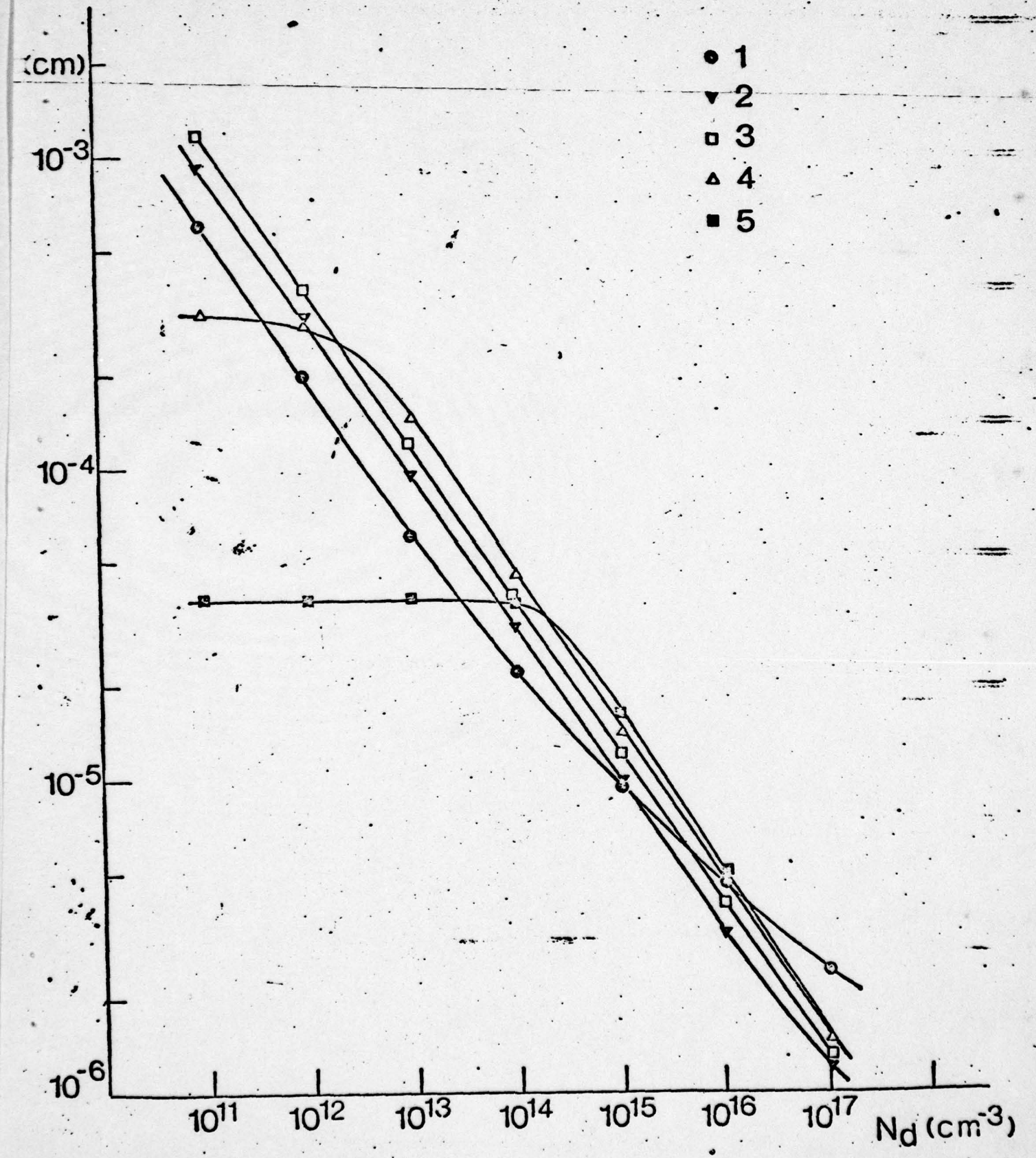
(cm)
$10^{-3}$
$10^{-4}$
$10^{-5}$
$10^{-6}$
1
2
3
4
5
$10^{11}$
$10^{12}$
$10^{13}$
$10^{14}$
$10^{15}$
$10^{16}$
$10^{17}$
$N_d$ ($cm^{-3}$)

Fig 2

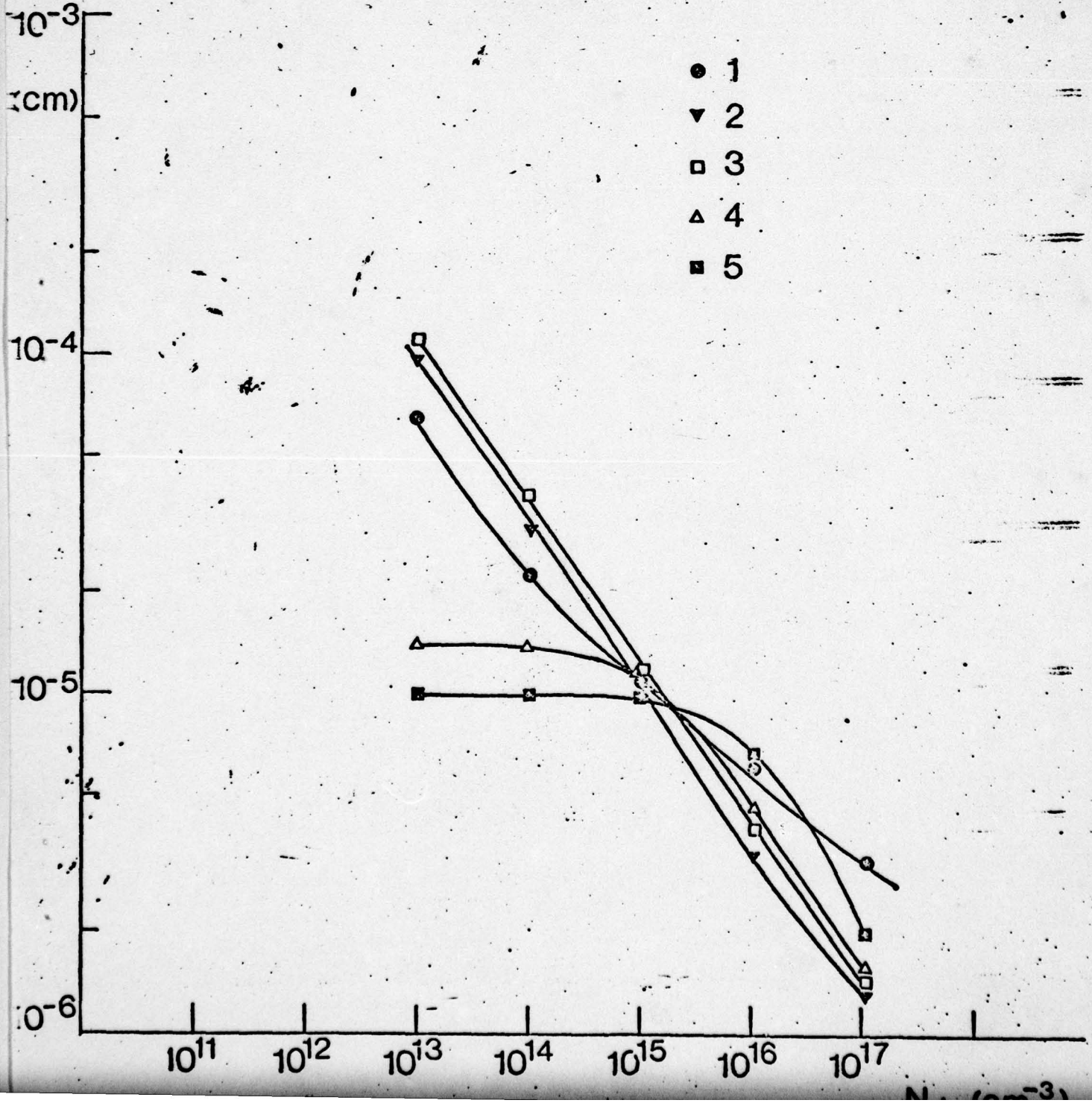

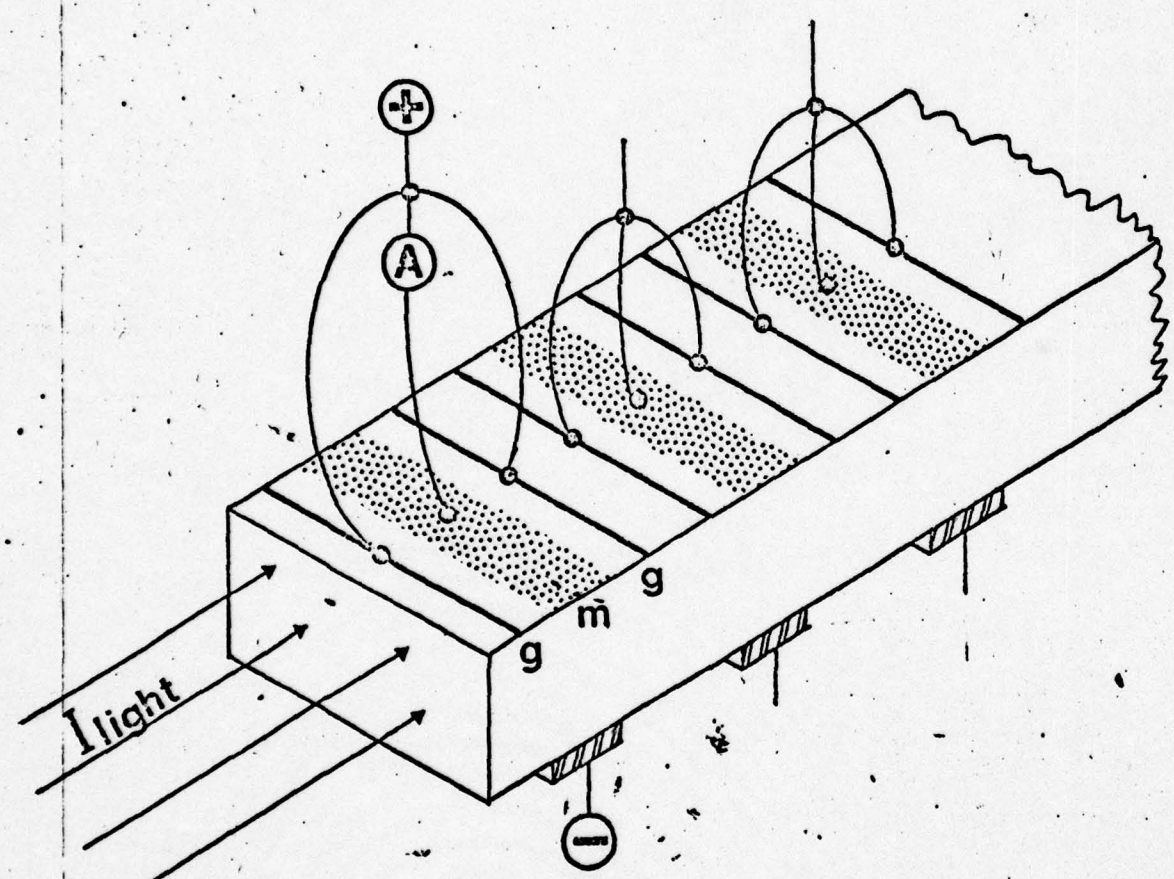


Fig.3

Appendix C

JOURNAL DE PHYSIQUE *Colloque C6, supplément au n°6, tome 40, juin 1979, page C6-207*

# APPLICATION OF DISLOCATION-INDUCED ELECTRIC POTENTIALS IN Si AND Ge*

S. Mil'shtein

*Department of Physics, Faculty of Natural Sciences, Ben Gurion University, Beer-Sheva, Israel*

Résumé.- On examine la barrière électrique (DEB) créée par une dislocation dans les semiconducteurs du point de vue de la recherche. En analysant la dépendance de la température du DEB, on obtient des résultats qualitatifs nouveaux sur les niveaux d'énergie dans les dislocations. On propose la possibilité de déterminer la densité des dislocations à l'aide de mesures électriques. Un modèle de dislocation isolée et des circuits monolitiques basés sur elle, sont discutés.

Abstract.- Utilization of dislocation electric barrier (DEB) in semiconductors for fundamental research purposes, as well as DEB device application is considered. Analyzing the DEB temperature dependence new qualitative information on dislocation energy states is obtained. Determination of dislocation density by electrical measurements is proposed. Model of single dislocation and monolithic circuits based on it are discussed.

1. Introduction.- From the very beginning the progress of semiconductor electronics was connected with studies of impurities in semiconductor crystals. The same situation now exists concerning investigations on dislocations. In comparison with impurities the role played by dislocations in crystals is no less substantial. The electric potential due to the point defect (impurity) drops with a distance r like 1/r, but DEB drops like $\ell n\, r$. Therefore, in the case of dislocation we will have an extensive electric field.

The presence of DEB in semiconductors causes the dislocation influence on their conductivity /1-2/, electron mean path /3-4/, carrier's lifetime /5-6/, optical properties /7-8/, etc...

The modern trend in microelectronics towards higher density of devices leads to a situation where the dislocations play a significant role. Even for devices of an active area of only 100 $(\mu m)^2$, a crystal material of say $10^6$ dislocations per $cm^2$ puts an average of one dislocation on every junction surface. As a result of growing, diffusion, implantation, etc.. the process-generated dislocation densities are often even higher than the figure of $10^3$ $cm^{-3}$ quoted for "good" crystal. But even this number of dislocations has a bad affect on the monolithic circuit with the device-density of about $10^9$ elements per 1 $m^3$.

At the same time new devices based on dislocations are created /9-10/. Therefore, the DEB application, in our opinion, means in the first place utilization of these potentials in attempts to obtain new information about the dislocation. Secondly, it also implies device application of DEB.

2. Crystals with high dislocation density.- Let us discuss first, under which conditions the DEB exists in semiconductor crystals. The n-type Si is taken like an example. Considering the DEB due to the dislocation cluster in n-type silicon we used the electric neutrality equation for semiconductor which becomes electrically inhomogeneous after plastic deformation (S. Mil'shtein, A. Senderihin, unpublished).

Our model /11/ deals with two parts of the crystal : the undeformed, n-type conductivity part and p-type zone with high dislocation density of about $10^{10}$-$10^{11}$$cm^{-2}$. In practice the problem is reduced to finding the Fermi levels in both parts.

The difference in the position of the Fermi levels results in the bending of the bands, i.e., in the emergence of an electric potential barrier. Resolving the electric neutrality equation separately the n- and p-type parts of a crystal, we obtain the height of DEB dependent on temperature on the free carriers concentration and position of single dislocation acceptor or on the dislocation band. A dislocation acceptor level of 0.39 eV is assumed for Si.

Figure 1 illustrates the temperature dependence of the DEB in Si with various initial donor impurities concentration from $10^{11}cm^{-3}$ to $10^{16}cm^{-3}$ in plastically deformed n-type Si assuming single dislocation level at E = 0.39 eV, there could exist a DEB, whose height changes from 0.739 eV to 0.176 eV with the rise of temperature from -200°C to +200°C. When the presence of empty dislocation band of 0.39-0.2 eV is taken into account, the potential barrier decreases form 0.95 eV to about 0.2 eV in the same temperature range.

* Supported by the U.S. Air Force

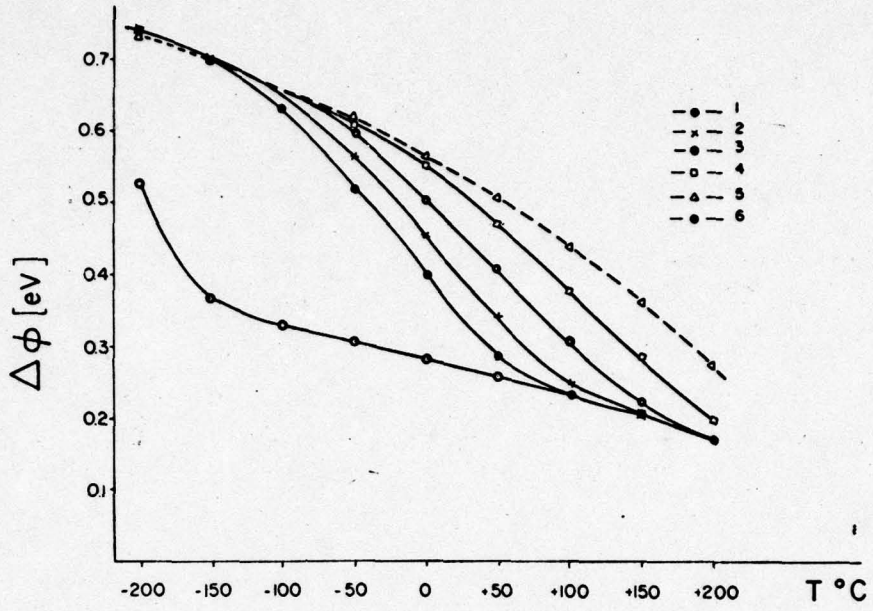


Fig. 1 : DEB temperature dependence in Si for the case of single dislocation level and concentrations $1\text{-}10^{11}cm^{-3}$, $2\text{-}10^{12}cm^{-3}$, $3\text{-}10^{13}cm^{-3}$, $4\text{-}10^{14}cm^{-3}$, $5\text{-}10^{15}cm^{-3}$, $6\text{-}10^{16}cm^{-3}$.

We can see that the DEB of dislocation cluster exists, in a wide temperature range, in crystal with a varied concentration of impurities.

We made an attempt to obtain the qualitative information about dislocation energy states from the DEB temperature dependences. It follows from our calculations, that in a case of the empty dislocation band the height of DEB is about 0.5-0.6 eV in crystals with an initial donor concentration of $10^{13}$-$10^{15}cm^{-3}$. This is approximately twice the value measured by us on identical crystals at room temperature /11/. At low temperature the barrier almost reaches the magnitude of the forbidden bandwidth. These exaggerated values for the electric potentials can be obtained, if it is conjectured, that instead of a empty dislocation band it's bottom taken into account ($E_a$ = 0.2 eV or even more shallow level) . Our calculations were in agreement with experiment /11-12/ if deep-lying single levels or more than half-filled dislocation band had been taken into account, i.e. 0.35-0.39 eV are the limits for Fermi level.

In the case of the empty dislocation band at temperature below -150°C the DEB becomes so high that Fermi level in the nondeformed n-type part of Si touched the bottom of conduction band, and, in the p-type it passes through the values of the dislocation band. In that case the voltage-current characteristics must resemble the characteristics of tunnel diodes. The tunneling effect has, however, not been observed by anyone, even though low temperature measurements were made on bicrystals /13/ and on heavily dislocated Si /12/, where the density of dislocation acceptors up to $10^{17}cm^{-3}$ has been indicated. This fact enabled us to assume, that the deep-lying dislocation band, with width of about several hundredths of an electron-volt, is involved in DEB emergence.

The method described above can also be used on n-type Ge and p-type materials as well. In hole materials the p-$p^+$ type barriers can be computed.

Let us discuss one more example of DEB applications for purposes of fundamental research. The p-n junctions, formed by the dislocation cluster has capacity per $cm^2$ (C) which we measured by special bridge (model 4270A Hewlett Packard) at room temperature. The DEB height $\phi$ of about 0.3 eV was measured by methods developed in our recent work /11/.

Figure 2 presents $C^2$ versus reverse bias voltage V. In case of $q\phi >> kT$ we can use the model of abrupt p-n in action. Therefore, capacitance measurements /14/ furnish a simple way of determining the density of acceptors in a deformed part of the crystal, i.e., the dislocation density :

$$\phi - V = \frac{\varepsilon e}{8\pi C^2} \frac{N_d \cdot N_a}{N_d + N_a} , \qquad (1)$$

Using equation (1) for Si with $N_a \sim 10^{14}cm^{-3}$, we find the density of dislocation acceptors of about

$2x10^{15}$ and that is equivalent to the dislocation density $N_{dis} \simeq 1.3x10^{9}$ cm$^{-2}$. Control measurements by the aid of the electron microscope revealed $N_{dis}$ of about $8.6x10^{8}$ cm$^{2}$, which agrees well with our calculation.

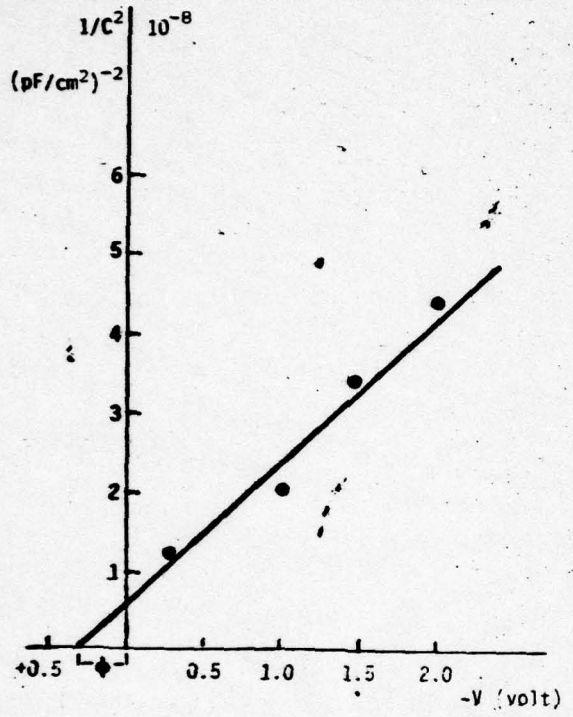


Fig. 2 : $C^2$ dependence on reverse bias voltage.

The semiconductor devices bases on dislocations /9-10/ have substantially improved their characteristics and are especially advantageous as regards their temperature stability. They recover after both electrical and thermal breakdowns. Their production technology is very simple because neither diffusion of dopants nor electrical processing are necessary. This technology can be used for producing diodes, as well as for different types of semiconductors devices (photocells, field effect transistors, etc.). It must be pointed out, however, that the question of their application is still open because their noise parameters (especially 1/f noise) have still not been investigated.

It is proposed to produce the above semiconductor devices on dislocations introduced into the crystal by plastic deformation. Laser irradiation could be used to introduce dislocations. Thus, paper /15/ indicates that p-n junctions of a small area were obtained by the laser irradiation of a silicon plate. True, such irradiation /15/ burned impurities into the crystal and the rectification obtained cannot be ascribed to the dislocation alone. It can however be expected that laser irradiation, leading to melting and recrystallization of a small volume of the crystal and creating dislocations, will be a cheap and accurate method of manufacturing devices bases on dislocations.

3. Crystals containing single dislocations.- The single dislocation electrical barrier (SDEB) in Si and Ge can be obtained solving the Poisson's equation in cylindric coordinates :

$$\frac{1}{r}\frac{d}{dr}\left(r\frac{d\phi}{dr}\right) = -\frac{1}{\varepsilon\varepsilon_0} qn_0(1 - e^{q\phi/kT}), \qquad (2)$$

where $\phi$ - is a potential of SDEB, under combined boundary conditions :

$$r = r_0 \quad \left.\frac{d\phi}{dr}\right|_{r=r_0} = \lambda r_0 \qquad (3a)$$

$$r \to \infty \quad \phi = 0 \qquad (3b)$$

where $\lambda$ - is the density of charge at the dislocation core.

A model has been proposed by us (S. Mil'shtein, A. Senderihin, unpublished) in which the dislocation charge is not concentrated at the line, but is spread throughout the cylinder of the radius $r_0$ of about three lattice constants. Such an approach allows us to operate with a finite value of the electrostatic potential. In approximation $q\phi >> kT$ and $q\phi << kT$ two analytical solutions can be obtained. Joining these two representations quite accurately, we have a form of SDEB in the considered area.

Figure 3 shows the 60° - SDEB in Si with various donor concentration. As it can be seen from figure 1, with changing of donor concentration from $10^{11}$cm$^{-3}$ to $10^{18}$cm$^{-3}$ the SDEB drops from 0.22 eV to 0.03 eV at room temperature. The distance at which the potential actually turns into nil is in to shown limits : from $7x10^{-3}$ cm to $10^{-6}$ cm.

Figure 4 presents 60° - SDEB temperature dependence in Si with $N_d = 10^{13}$cm$^{-3}$ with decrease in temperature from +30°C to -220°C the SDEB increases from 0.17 eV to 0.42 eV. All the curves turn to nil at the distance $5x10^{-4}$ m.

We can see from figures 3 and 4 that in n-type Si with various concentrations of impurities exist an extensive SDEB in wide temperature range. The same computation can be done for n-type Ge and p-type materials as well. From the presented curves (Figs. 3 and 4) we obtained an additional information about the structure of SDEB. Our calculation shows that the electric potential drops logarithmically on the distance $r \simeq 0.65$ $L_D$ ($L_D$ - Debye screening length) and then decreases

On the basis of our calculations and measurements which were previously carried out by means of micro probes an equivalent diagram of a charged dislocation has been drawn (cf. Fig. 5). Our calculation shows that a p-region near the dislocation line does not exist, and it is just a strongly intrinsic area almost up to room temperatures and impurity concentration from $10^{11}cm^{-3}$ to $10^{18}cm^{-3}$. It has been proved by our experiments that, when current is passed along the dislocation, rectifying processes are developed only at the edges of the cylindrical i-n structure. The values of the running currents did not change when the dislocation length was changed by several orders of magnitude. The violent spreading of the current is probably due to the high resistance of the p-region. On the diagram this resistance is denoted by $R_i$. When coltage is applied to the dislocation ends, the current runs through the equivalent resistance $R_n$ (the resistance of area-n) and the diodes $D_1$ and $D_2$ connected opposite to each other. The notion about dislocation as about a line with a distributed resistance and capacitance (delay lines) seems therefore to be not quite correct. Carriers injected by light or by an electrical field will not pass through the dislocation delay line but through the diodes loop because the resistance $R_i$ is high and comprises, to our assessment, $10^{10}$ - $10^{11}$ohm.

The electrical equivalent scheme of single dislocation (by point lines) can be usefully utilized in monolithic circuits, some of them given like examples on figure 6 : a) full-wave rectifier, b) double diode clipper, c) gate "AND", d) gate "OR". It is beyond the scope of this work any discussion on electronic effects due to frequency and level of signals and on the many various types of circuits as well.

It must be pointed out that the introduction of single dislocations via mechanical deformation (scratching and bending) of the crystals, does not seem to be the best technology for mass-production of electronic devices. While it appears that epitaxial growth is eventually going to be the proper method to obtain misfit dislocations in a controllable manner. There is no satisfactory technology available at the moment.

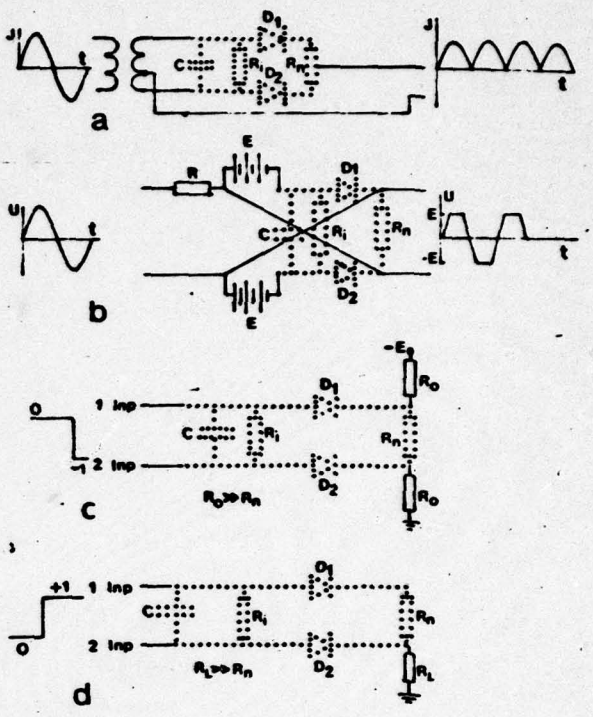


Fig. 6 : Possible application (several examples) of the single dislocation in microelectronics : a) Full-wave rectifier, b) double-diode clipper, c) gate "AND", d) gate "OR".

## References


/1/ Gerlach, E., Rantenberg, M., Phys. Status Solidi B67 (1975) 519.

/2/ Miles, M.J., Collins, Ch., J. Appl. Phys., 42 (1971) 5644.

/3/ Pödor, B., Acta Tech. Acad. Sci. Hung., 80 (1971) 231.

/4/ Milevskii, L., Zolotuchin, A., JETP Lett., 19 (1974) 255.

/5/ Figielski, E., Phys. Status Solidi, 9 (1965) 555.

/6/ Jastrebska, M., Figielski, T., Phys. Status Solidi, 14 (1966) 381.

/7/ Kamienicky, E., Phys. Status Solidi A4 (1971) 257.

/8/ Mil'shtein, S., Yakobi, B., Phys. Lett. A54 (1975) 6,465.

/9/ Mil'shtein, S., U.S.A., Patent 4, 005, 523.

/10/ Mil'shtein, S., IEEE Transact. Electron. Devices 1184, Oct. 1976.

/11/ Mil'shtein, S., J. Appl. Phys. 46 (1975) 9, 3894.

/12/ Eremenko, V., Nikitenko, V., and Yakimov, E., Sov. Phys. - JETP, 40 (1974) 3, 570.

/13/ Hamakawa, Yo, Yamaguchi, J., Japan. J. Appl. Phys., 1 (1962) 6, 334.

/14/ McKelvey, J., Solid State and Semiconductor Physics, (New York, Harper & Row) 1966, p. 404.

/15/ Fairfield, J., Shwuttke, G., Solid State Electron. 11 (1968) 12, 1175.

exponentially.

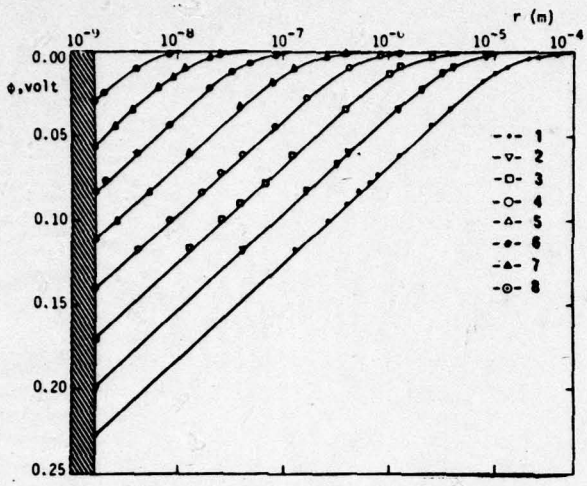


Fig. 3 : SDEB dependence on the donor concentration in Si : 1-$10^{11}cm^{-3}$, 2-$10^{12}cm^{-3}$, 3-$10^{13}cm^{-3}$, 4-$10^{14}cm^{-3}$, 5-$10^{15}cm^{-3}$, 6-$10^{16}cm^{-3}$, 7-$10^{17}cm^{-3}$, 8-$10^{18}cm^{-3}$.

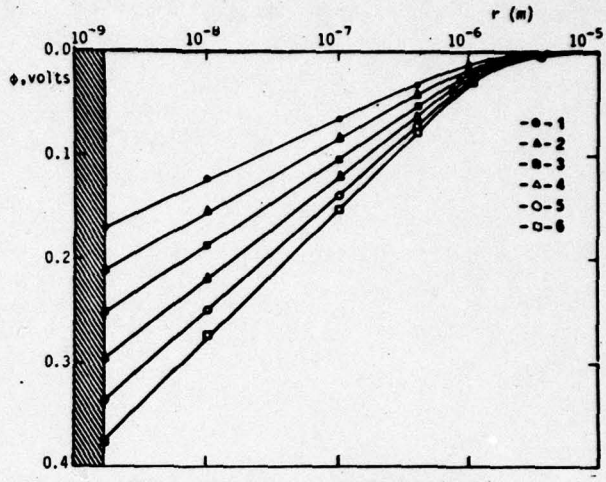


Fig. 4 : SDEB temperature dependence in Si, 1 -+30°C, 2 - -20°C, 3 - -70°C, 4 - -120°C, 5 - -170°C, 6 - -220°C.

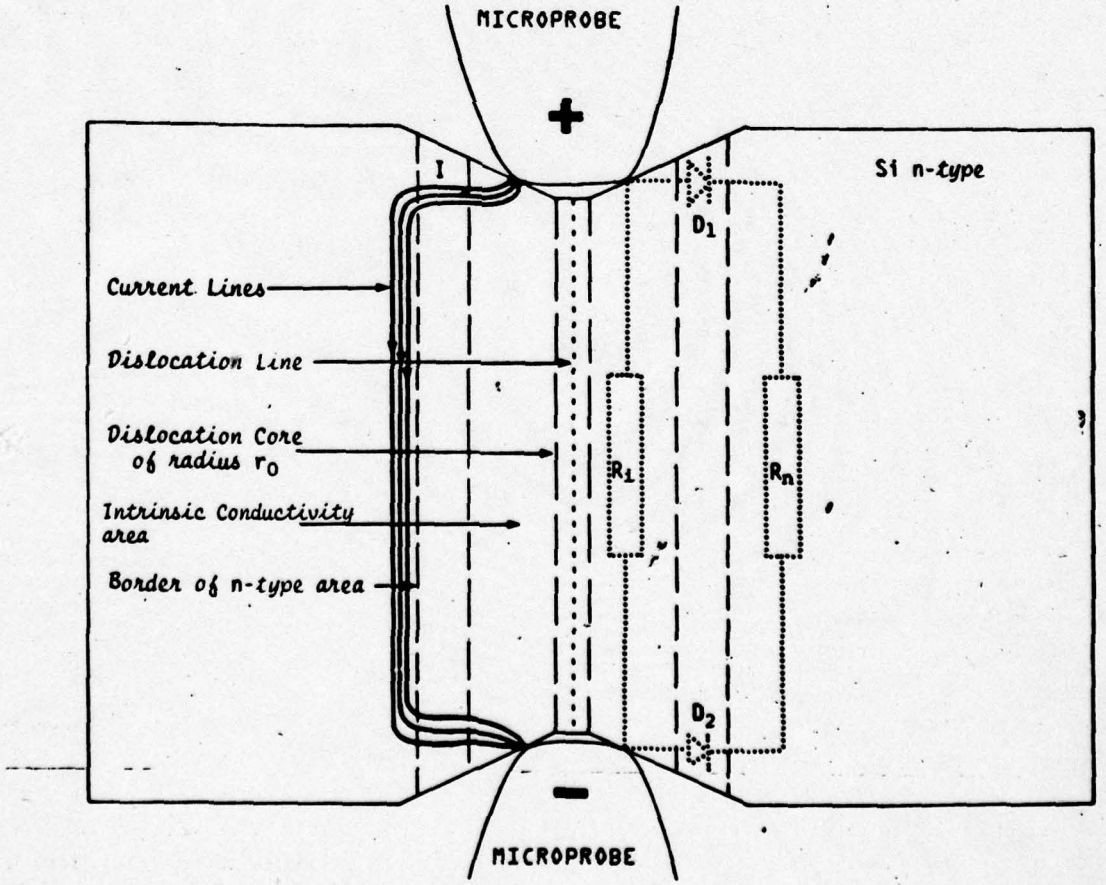


Fig. 5 : Model of charged single dislocation

2

# Appendix D

## MODEL OF SINGLE CHARGED DISLOCATION IN TETRAVALENT SEMICONDUCTORS*

S. Mil'shtein, A. Senderichin

Department of Physics, Faculty of Natural Sciences,

Ben-Gurion University, Beer-Sheva, Israel

**Abstract**

Electric field around a single edge dislocation in semiconductors is analyzed taking into account the screening effect of free electrons. Theoretical calculations were made on temperature dependent single dislocation electrical barrier (SDEB). SDEB dependence on concentration of impurities is computed. The existence of a very narrow inverse layer around a single dislocation is strongly limited by the temperature and donor concentration. The validity of Read's dislocation model is discussed and the new model is considered.

Submitted to Phys. Rev.

* Supported by U.S. Air Force

## Introduction

Investigation of single edge type dislocations in semiconductors enabled us to observe a number of electrical [1-2] optical [3-4] and diffraction effects [5-6] resulting from the presence of an electrical field around such dislocations.

The classical consideration of local electrical fields due to dislocations in semiconductors by Read [7] ignores the screening effect of free carriers and is therefore valid only for heavily doped crystals at low temperatures. Solving the Poisson's equation for a charged dislocation line Schröter and Labush [ 8 ] established the electrical potential associated with the dislocation. These authors, using the approximations for $q\varphi \gg KT$ and for $q\varphi \ll KT$, obtained a general solution of Poisson's equation for the crystal's region near the dislocation and one far from it respectively. There is yet no strict demarcation between these two regions. The possibility of observing the effect of single dislocations on the local change of the electrical properties as well as other features of semiconductor devices is, perhaps, associated with the dimension and the form of the electrical anomalous regions and with the shape of the potential drop.

The purpose of this work is to obtain more detailed information on the shape of the potential field and on its dependence on the type of dislocations, crystal parameters and temperature.

Poisson's equation has been solved analytically for the far away ($q\varphi \ll KT$) and near by ($q\varphi \gg KT$) crystal regions around the

charged dislocation line. Both solutions are joined under chosen boundary conditions. The piece-continuous function has been obtained from this solution and the coefficients of one were determined by numerical methods. Based on these solutions a model of a charged dislocation is discussed.

## Theory

Our model deals with the dislocation charge which is not concentrated on the line but is spread throughout the cylinder having a radius $r_0 = 3a$, where $a$ is the lattice constant. The chosen cylinder size seems to be reasonable from the theoretical point of view and from the experimental point of view lies beyond the sensitivity of the electron microscopy methods used in the experiment [ 9 ]. Such an approach allows us to operate with a finite value of the electrostatic potential.

Let us consider a negatively charged dislocation core in n-type material. For a p-type semiconductor the consideration will be similar. The size of the cylindrical area in which a dislocation effect exists is $r \ll \ell$, where $\ell$ is the length of the dislocation line. On other words only long sections of dislocations have been considered. This region is supposed to be far enough from the crystal surface, i.e., effect of the charge located at the surface is not available. Only screening by means of charged donors and free electrons is taken into account in a case of single dislocation in n-type material. When the value of SDEB is obtained the charge distribution including both free electrons and holes is calculated.

Poisson's equation in cylindrical coordinates can be written as:

$$\frac{1}{r}\frac{d}{dr}\left(r\frac{d\varphi}{dr}\right) = -\frac{1}{\varepsilon\varepsilon_0}\left[qN_0\left(1 - e^{q\varphi/KT}\right)\right] \qquad (1)$$

The designations are generally accepted. The spatially distributed charge of donors and of free electrons on the right side of the equation is recorded.

Mathematical statement of the problem includes two mixed boundary conditions for solution of this second-order differential equation:

1) the electric field at the surface of a charged cylindrical core determined by the charge density per unit length $\lambda$:

$$-\left.\frac{d\varphi}{dr}\right|_{r=r_0} = \frac{\lambda}{2\pi\varepsilon\varepsilon_0 r_0} \tag{2}$$

2) the electric potential at infinity is assumed to be zero:

$$\varphi|_{r\to\infty} = 0 . \tag{3}$$

Let us use nondimensional parameters:

$$\tilde{\varphi} = \frac{q\varphi}{KT} ; \quad \tilde{r} = \frac{r}{L_D} ; \quad \tilde{\lambda} = \frac{\lambda}{2\pi q n_0 r_0^2} \tag{4}$$

where $L_D$ is Debye screening length.
Equation (1) will then acquire the form:

$$\frac{1}{\tilde{r}} \frac{d}{d\tilde{r}} \left(\tilde{r} \frac{d\tilde{\varphi}}{d\tilde{r}}\right) = -\left(1 - e^{\tilde{\varphi}}\right) \tag{5}$$

with boundary conditions:

$$\begin{aligned} &\tilde{r} = \tilde{r}_0 && -\frac{d\tilde{\varphi}}{d\tilde{r}} = \tilde{\lambda}\, \tilde{r}_0 \\ &\tilde{r} \to \infty && \tilde{\varphi} = 0 \end{aligned} \tag{6}$$

The tilda sign (~) will henceforth be omitted. Nonlinear equations (1),

(5) have no analytical solution for the considered region $\in r_0, \infty$ but it can be linearized for two parts of the area and the two representations will be joined. Near the core of the dislocation $|\varphi| >> 1$ and $\varphi < 0$, therefore $e^{\varphi} << 1$. The right side of equation (5) is equal to $-1$, and the solution will be:

$$\varphi_I = -\frac{r^2}{2} + C_1 \ln r + C_2 \tag{7}$$

By using the condition (6) the constant $C_1$ is defined

$$\varphi_I = -\frac{r^2}{4} + r_0^2 \left(\frac{1}{2} - \lambda\right) \ln r + C_2 \tag{8}$$

For regions far away from the dislocation $\varphi << 1$ and the exponent on the right side of equation (5) can be expanded into a series. The right side of the equation will then equal $\varphi$ and the solution will take the form:

$$\varphi_{II} = C_4 \cdot I_0(r) + C_3 \cdot K_0(r) \tag{9}$$

where $I_0$ and $K_0$ are Bessel's functions of the first and of the third kind respectively. The latter is a Hankel function. By using the second boundary condition (6) we obtain:

$$\varphi_{II} = C_3 \cdot K_0(r) \tag{10}$$

The Hankel function for large $r$ can be expressed in asymptotic form:

$$\varphi_{II} = C_3 \sqrt{\frac{\pi}{2r}}\, e^{-r} \tag{11}$$

Solutions (8) and (11) are joined at some point $r_1$ if the following conditions are met as we approach this point from the left and from the right:

$$\varphi_I(r_1) = \varphi_{II}(r_1) \tag{12}$$

$$\frac{d\varphi_I(r_1)}{dr} = \frac{d\varphi_{II}(r_1)}{dr} \tag{13}$$

$$\frac{d^2\varphi_I(r_1)}{dr^2} = \frac{d^2\varphi_{II}(r_1)}{dr^2} \tag{14}$$

Solving the system of equations (12)-(14) we can find the coordinate $r_1$ and the two constants $C_2$, $C_3$. Combining (13) with (14) a nonlinear algebraic equation in $r_1$ was obtained:

$$\left[\frac{r_1^2}{2} + r_0(\lambda - \frac{1}{2})\right]\cdot\left[1 + \frac{1}{4r_1^2}\right] + r_1\left[1 + \frac{1}{2r_1}\right] = 0 \tag{15}$$

After determining $r_1$ from equation (15) we substitute it into the system of equations (12)-(14) and find the constants $C_2$ and $C_3$. Thus the equation (5) at mixed boundary conditions (6) is solved.

The reported solution of the problem can be considered as "zero approximation", since carrying out an integration of the differential equation the range of integration was divided only in two sections and the right side of the equation was not used in the complete form. By increasing a number of sections and using the iteration method, the accuracy of "zero approximation" can be estimated and a stability of the solution can be proved. According to previous data the error in determination of a potential at the surface core does not exceed 2-3% and then the zero approximation is exact enough. Having a ~~quite~~ faithful solution of equation (5) we can now define the effect of dislocation type, resistivity

and temperature of semiconductor upon the drop in potential around the dislocation line.

The boundary conditions (2) (6) are determined by means of charge density $\lambda$, that is a function of the filling factor $f$ and of the dislocation type [ 7]:

$$\lambda = \frac{q\, f \cdot \sin\alpha}{0.866 \cdot a_1} \quad (\frac{cul}{m}) \qquad (16)$$

where $\alpha$ - is an angle between the dislocation and Burger's vector.

Based on Read model [ 7] the filling factor has been calculated in approximation of "Fermi statistics".

The presence of deep acceptor states about 0.2 eV and 0.4 eV above the valence band for Ge and Si respectively were assumed. The selected acceptor states comply with numerous theoretical and experimental results [10-11]. The shape of the electrical potential indicates that there is a depletion layer near the dislocation line. In a range of low densities and of high temperatures an inversion layer arises and p-n junction if formed.

Results

Fig.1 presents sixty degree single dislocation electrical barrier ($60^{\circ}$-SDEB) dependence on donor concentration $N_o$ in Si at room temperature. As is shown in Fig.1 the SDEB decreases from 0.22 eV to 0.03 eV when the donor concentration varies from $10^{11}cm^{-3}$ to $10^{18}cm^{-3}$. The distance which the potential approximately reaches zero changes from $10^{-6}$ to $10^{-8}m$ with $N_o$ decreasing.

The same dependence for $60^{\circ}$ dislocation in Ge is presented in Fig.2.

When $N_o$ changed from $10^{13}cm^{-3}$ to $10^{17}cm^{-3}$ SDEB decreases from 0.21 eV to 0.07 eV at room temperature. The distance which the potential reaches approximately zero decreases from $5.10^{-6}m$ to $5.10^{-8}m$. One can see from the equation (8) that the electrical potential depends on $\lambda$ or, which is the same, on the number of sites along a dislocation line. For various types of dislocations the number of free sites or "dangling" bonds per unit length would change. Table 1 presents the calculated electrical potential at the core of various dislocation types in Si and Ge at room temperature.

Table 1

| Dislocation type | $\varphi$ (v) Si, $N_o = 10^{13}cm^{-3}$ | $\varphi$ (v) Ge, $N_o = 10^{14}\ m^{-3}$ |
|---|---|---|
| $30^o$ | 0.099 | 0.100 |
| $60^o$ | 0.170 | 0.179 |
| $90^o$ | 0.190 | 0.205 |

Fig.3 shows the temperature dependence of $60^o$-SDEB in Si with $N_o = 10^{13}cm^{-3}$. When the temperature decreases from $300^oK$ to $50^oK$, the SDEB increases from 0.17 eV to 0.37 eV. All the curves approach zero at the distance about $10^{-5}m$. With decreasing temperature the slope of the curves slightly increases.

Fig.4 presents the temperature dependence of $60^o$-SDEB in Ge with $N_o = 10^{14}cm^{-3}$. The same temperature dependence as in the Si case is found. The changes in temperature from $300^oK$ to $50^oK$ results in changes in SDEB from 0.18 eV to 0.32 eV respectively. Knowing SDEB quite precisely

we calculated the distribution of free holes in the vicinity of the dislocation core.

Fig.5 presents the temperature dependent radius of p-type cylinder versus $N_o$ in Si. One can see from Fig.5 that below room temperature this radius $r_p$ is small. Even in Si with $N_o = 10^{12}cm^{-3}$ $r_p$ is less than $10^{-7}m$. This radius $r_p$ decreases proportionally when increasing the concentration $N_o$, while $r_p$ increases by three orders of magnitude with the temperature rising from 250°K to 400°K.

The same dependence of $r_p$ in Ge is shown in Fig.6. For temperatures $T < 300^oK$ $r_p < 10^{-7}m$. We did not raise the temperature as much as in the case of Si. In the temperature range from 200°K up to 400°K, $r_p$ changes by two orders of magnitude. In a wide range of concentrations and temperatures the validity of Read theory was considered. For this purpose we compared $r_1$ from equation (15) with the radius of Read cylinder $r_c$ which is given by

$$r_c = \sqrt{\frac{f}{\pi n_o c}} \qquad (17)$$

where c - the distance between captured electrons. This comparison will be discussed below.

In Fig.7 the model of a single charge dislocation is sketched. The equivalent scheme of the dislocation is also given.

Discussion

The general solution for the problem of finding the electrical potential distribution around a single charge dislocation line is obtained.

The solution enables us to relate an electrical potential at the dislocation core to the dislocation type, determined by angle $\alpha$ between the dislocation line and the Burgers' vector, concentration of donors $N_o$ and temperature T. The calculation shows that changing $\alpha$ from $30^o$ to $90^o$ decreases (see eq.16) the number of sites per unit of dislocation line approximately by factor 2; that means a proportional increasing of the electrical potential at the core. In n-type Si and Ge the electrical potential at the core strongly depends on $\lambda$-charge density per unit length, determined in their turn by the filling factor f (see eq.16). This potential depends also on the radius of the core (see boundary conditions eqs.2 and 3). The filling factor is calculated in approximation of"Fermi-statistics" and increases as temperature decreases. The potential at the core (see Fig.3 and Fig.4) rises by factor 1.5 as temperature decreases from $300^oK$ to $50^oK$ and reaches for Ge 0.32 V. Another factor influencing the dislocation potential is the radius of the charged core selected by us to be equal to $r_o = 3a$, where a is the lattice constant. Previous calculations have shown that the change of the core's dimensions has a less pronounced influence on the SDEB than the choosen statistics approximation.

2.

The distance on which the potential is still perceptible decreases with the donor's concentration increasing (see Fig.1 and Fig.2). At the same time the potential gradient remains constant. The change of donor concentration of $N_o$ in a wide range from the "intrinsic concentration" (for Ge $10^{13}cm^{-3}$ and for Si $10^{11}cm^{-3}$) to the "degenerate one" ($10^{17}$ - $10^{18}cm^{-3}$) results in the distance decreasing from $10^{-4}m$ to $10^{-8}m$, i.e. for Si on

four orders of magnitude and for Ge from $4.10^{-5}$cm to $4.10^{-7}$m, i.e. on two orders of magnitude. The value of the potential at the core in the two cases does not lie outside the range 0.25 eV which is in agreement with the results of Figielsky [12]. Therefore in Si and Ge there may exist a perceptible SDEB which can be measured by the aid of sharp microprobes [13-14] in the crystals with $N_o$ up to $10^{15}cm^{-3}$ and by the aid of an electron beam [9] in the specimens with $N_o$ up to $10^{18}cm^{-3}$.

Investigating the temperature dependence of J-V characteristics, Eremenko et al.[15] established a much higher electric potential $\varphi$ = 0.4 V at the distance of 1μ from a dislocation line. This value would result at the dislocation core the potential step of about 5 V and the electric field must destroy the Si crystals. On the other hand, the slope of the current-voltage characteristics presented in this work [15] shows the existence of a much smaller potential step. Therefore the presented results [16] are contradicting ones. This contradiction seems to be a result of temperature measurements performed on non-protected pressure point contacts. It is well known that heating causes the appearance of an oxidation layer at a metal-semiconductor interface which can lead to rather confusing results.

3.

The SDEB temperature dependence (see Figs.1,2)on Si and Ge shows that with decreasing the temperature from $300^{o}K$ to $50^{o}K$ increase the absolute value of SDEB as well as slightly increasing the gradient of the potential. But all the curves converge at zero for Si at $r = 10^{-5}m$ and for Ge at $r = 10^{-6}m$. One can conclude that relatively "big"electrically anomalous areas around edge-types dislocations can be detected in a wide temperature range.

4.

In the classical consideration of SDEB made by Read [7] the free electron screening effect is neglected. Trying to understand the validity of Read's theory we compared the dimension of the so-called Read cylinder $r_c$ with the parameter $r_1$ of our calculations. Let us recall that $r_1$ is a point where both the solutions $\varphi_I(r)$ and $\varphi_{II}(r)$ were joined. The condition $r_1 > r_c$ means that the point at the distance $r_c$ still belongs to the branch $\varphi_I(x)$, where the contribution of electrons is not taken into account. On the contrary, the condition $r_1 < r_c$ means that the point at the distance of the Read cylinder already belongs to the function branch $\varphi_{II}(r)$ where we are taking into account the free electron's screening effect. The calculations show that in a wide concentration range and up to very low temperatures the Read model is not fulfilled because $r_1 < r_c$ in the considered range. Neglecting the screening by free electrons, Read assumed the existence of an electric field E within the cylinder and a zero electric field outside the cylinder. This means there is a discontinuity in the electric field strength which can happen only if some internal charged surface exists. Such a situation in a real crystal is not physically feasible. Only for heavily doped semiconductors at low temperatures does the Read approximation seem to be valid.

5.

Calculating the charge distribution due to the SDEB, we found that near a single dislocation there exists a very narrow p-type cylinder layer whose radius $r_i$ decreases with the increasing donor concentration $N_o$ when the temperature increases from its minimum value to room temperature. The largest p-cylinder at room temperature is $10^{-7}$cm for both Si and Ge where

$N_o = 10^{12} cm^{-3}$ for the former and $N_o = 10^{14} cm^{-3}$ for the latter.

The rest of the anomalous area is"strongly intrinsic"and has a very high resistance [16]. That explains why the current injected by microprobes into an "i-pipe" spread out and does not flow along the i-type cylinder. Thus applying the voltage to the opposite edges of the dislocations of various lengths we did not find any difference in the resistance. Spreading out from the point where microprobe is mounted, carriers cross the i-n interface, where a strong rectification takes place. Now we can understand why the J-V characteristics of the "dislocation diodes" [12] have a slope resembling a Shottky i-n structure. It appears that the electrical model of a single edge-type dislocation described in the literature behaving like cylindrical p-n structure able to work as a delay line [17] is not quite correct. In terms of our equivalent scheme [16] there is a chain of two i-n diodes connected oppositely to each other. Carriers injected near the microprobe by light or by electric field would spread out from the cylinder, flow through the bulk and would come to the opposite side of the dislocation near the second microprobe.

In other words, the radius of the p-type cylinder is very small, its resistance $R_p$ is much larger than the resistance $R_i$ of the intrinsic layer. And there always works a shunt for $R_i$ which is the half-loop of two diodes and $R_n$. Therefore it seems impossible to perform simple AC or DC measurements of the conductivity along the charged dislocation.

The authors sincerely acknowledge the technical help of Mrs. T. Waksman. The authors also gratefully acknowledge the support of the Air Force Office of Scientific Research and EOARD who sponsored this work under grant AFOS-78-3526.

References

1. B.S. Lagowski, Phys. Status Solidi 5, 555 (1964).

2. F. Galsecchi, P. Gondi and F. Shintu, Nuovo Cimento B 58, 376 (1968).

3. A. Shynoweth, K. McKay, Phys. Rev., 102, 369 (1956).

4. S. Mil'shtein, submitted.

5. H. Matare and C. Laakso, Appl. Phys. Lett. 13, 216 (1968).

6. H. Matare, J. Appl. Phys. 30, 581 (1959).

7. W. Read, Phil Mag, 45, 775, 1119 (1954); 46 111 (1955).

8. R. Labush and W. Shröter, in the book "Lattice Defects in Semiconductors" Institute of Physics, London, 1974 p.56.

9. D. Darby, J. Mater. Sci. 12, 9, 1827 (1977).

10. R. Labush and R. Schettler, Phys. Status Solidi A, 9, 455 (1972).

11. R. Glaenzer, A. Jordan, Solid State Electr. 12, 247 (1969).

12. T. Figielsky, Physica Status Solidi, 9, 555 (1965).

13. S. Mil'shtein and V. Nikitenko, JETP Lett. 13, 233 (1971).

14. S. Mil'shtein and V. Nikitenko, Sov. - Phys. and Technic of Semiconductors, 6, 8, 13444 (1972).

15. V. Eremenko, V. Nikitenko and E. Yakimov, Sov. Phys. JETP, 40, 3, 570 (1975).

16. S. Mil'shtein, Proceedings of the Symposium on Dislocations in Tetrahedrally Coordinated Semiconductors, in press.

17. W. Bardsley, in book "Progress in Semiconductors" Wiley,, N-Y.1960 v.4, p. 157.

Figure Captions

Fig.1. The dimension of electric anomalous area due to $60^{\circ}$-dislocation in Si with various $N_o$ at room temperature.

1 - $10^{11}cm^{-3}$ 2 - $10^{12}cm^{-3}$ 3 - $10^{13}cm^{-3}$ 4 - $10^{14}cm^{-3}$ 5 - $10^{15}cm^{-3}$
6 - $10^{16}cm^{-3}$ 7 - $10^{17}cm^{-3}$ 8 - $10^{18}cm^{-3}$.

Fig.2. The dimension of electric anomalous area due to $60^{\circ}$-dislocation in Ge with various $N_o$ at room temperature.

1 - $10^{13}cm^{-3}$ 2 - $10^{14}cm^{-3}$ 3 - $10^{15}cm^{-3}$ 4 - $10^{16}cm^{-3}$ 5 - $10^{17}cm^{-3}$.

Fig.3. The $60^{\circ}$-SDEB temperature dependence in Si with $N_o = 10^{13}cm^{-3}$

1 - $300^{\circ}K$ 2 - $250^{\circ}K$ 3 - $200^{\circ}K$ 4 - $150^{\circ}K$ 5 - $100^{\circ}K$ 6 - $50^{\circ}K$.

Fig.4. the $60^{\circ}$-SDEB temperature dependence in Ge with $N_o = 10^{14}cm^{-3}$

1 - $300^{\circ}K$ 2 - $250^{\circ}K$ 3 - $200^{\circ}K$ 4 - $150^{\circ}K$ 5 - $100^{\circ}K$ 6 - $50^{\circ}K$.

Fig.5. The thickness of inversion layer around $60^{\circ}$-dislocation as a function of temperature and donor concentration in Si

1 - $400^{\circ}K$ 2 - $350^{\circ}K$ 3 - $300^{\circ}K$ 4 - $250^{\circ}K$.

Fig.6. The thichness of inversion layer around $60^{\circ}$-dislocation as a function of temperature and donor concentration in Ge

1 - $400^{\circ}K$ 2 - ~~$350^{\circ}K$~~ 3 - $300^{\circ}K$ 4 - $250^{\circ}K$ 5 - ~~$200^{\circ}K$~~.
$350^{\circ}K$ $200^{\circ}K$

Fig.7. The sketch of a dislocation tube and its equivalent scheme.

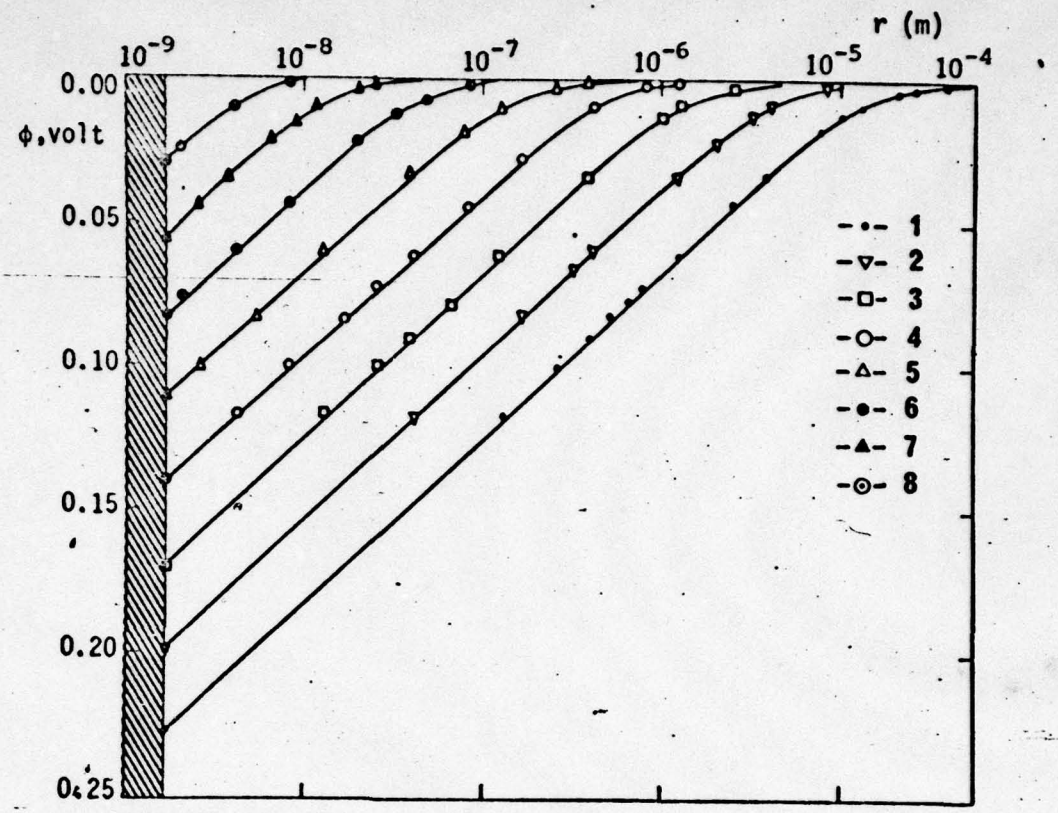
r (m)
$10^{-9}$
$10^{-8}$
$10^{-7}$
$10^{-6}$
$10^{-5}$
$10^{-4}$
0.00
φ,volt
0.05
0.10
0.15
0.20
0.25
1
2
3
4
5
6
7
8

Fig 1

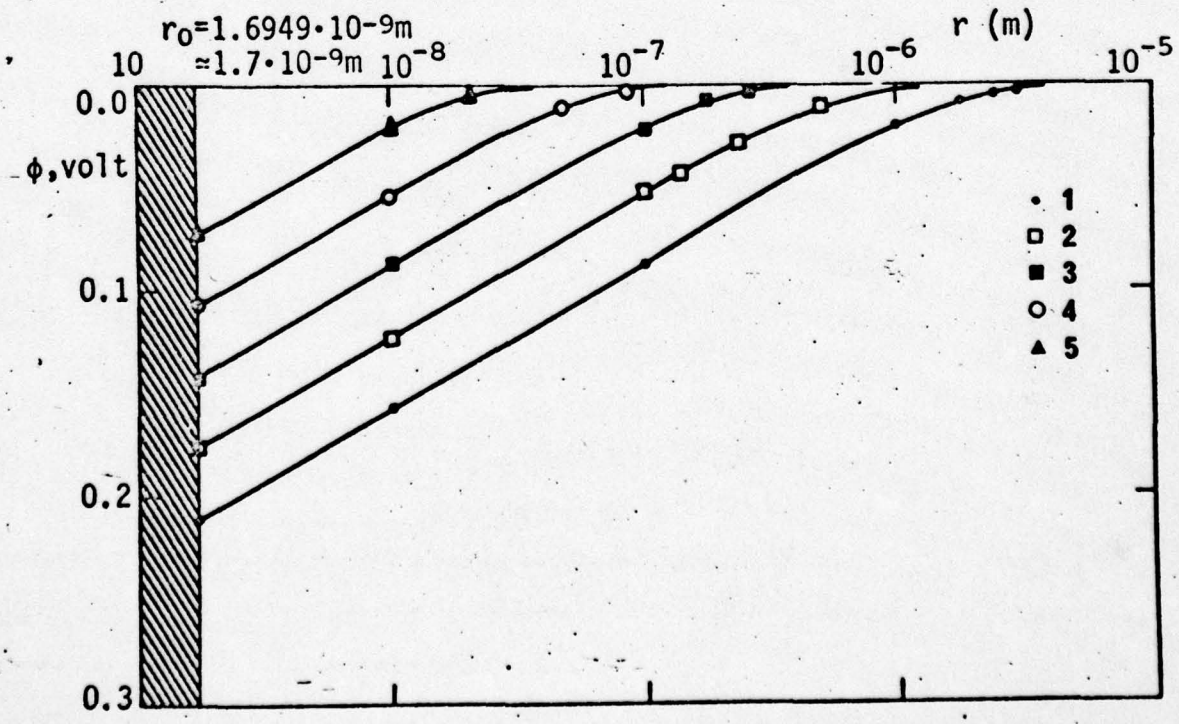
$r_0$=1.6949·10-9m
≈1.7·10-9m
r (m)
10
$10^{-8}$
$10^{-7}$
$10^{-6}$
$10^{-5}$
0.0
φ,volt
0.1
0.2
0.3
1
2
3
4
5

Fig 2

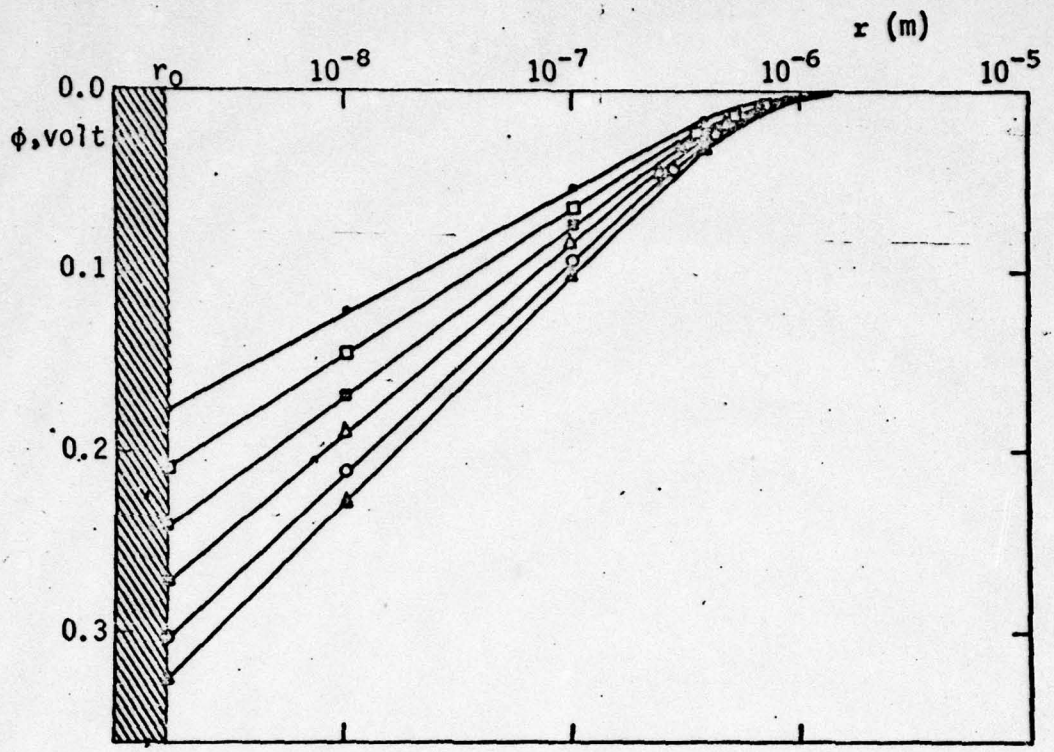
x (m)
$r_0$
$10^{-8}$
$10^{-7}$
$10^{-6}$
$10^{-5}$
0.0
φ,volt
0.1
0.2
0.3

Fig 4

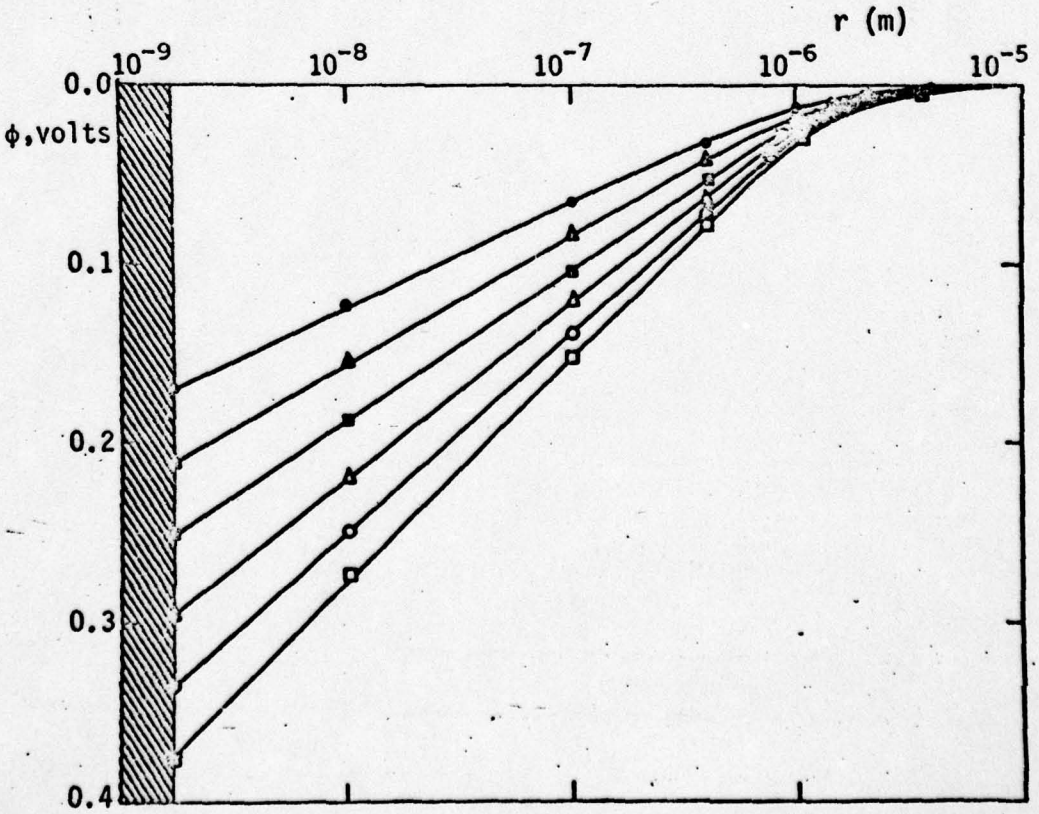
r (m)
$10^{-9}$
$10^{-8}$
$10^{-7}$
$10^{-6}$
$10^{-5}$
0.0
φ,volts
0.1
0.2
0.3
0.4

Fig 3

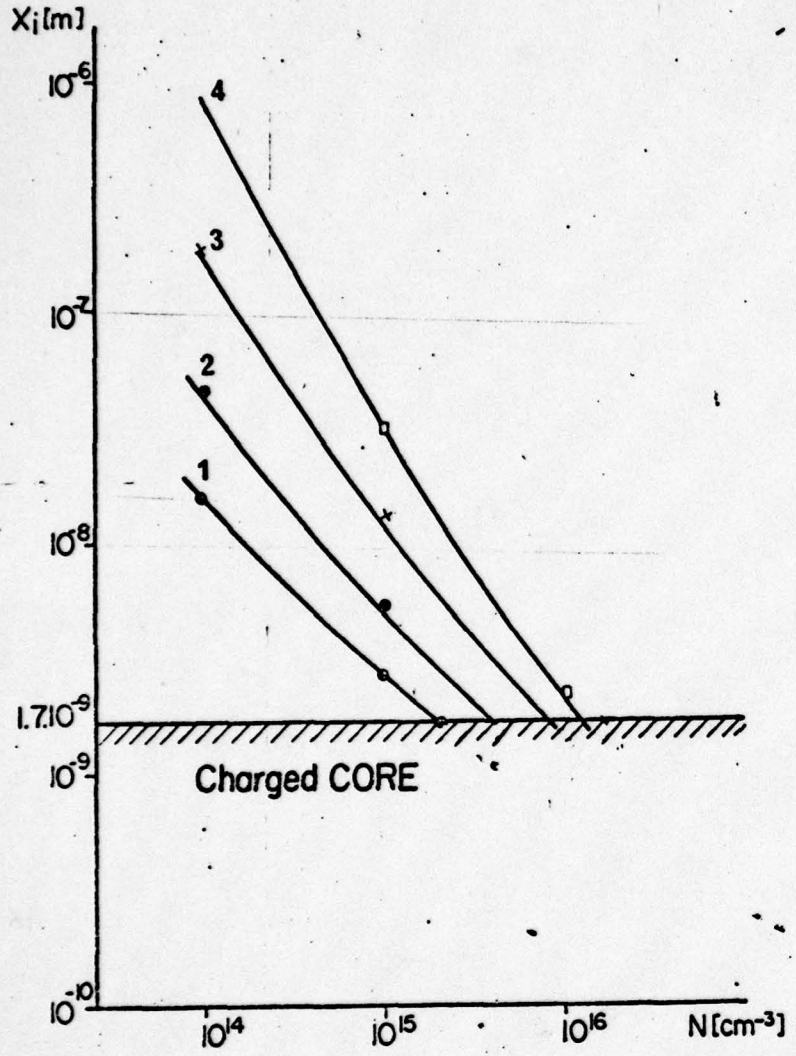
$X_i$[m]
$10^{-6}$
$10^{-7}$
$10^{-8}$
$1.7.10^{-9}$
$10^{-9}$
$10^{-10}$
4
3
2
1
Charged CORE
$10^{14}$
$10^{15}$
$10^{16}$
N[cm$^{-3}$]

Fig 6

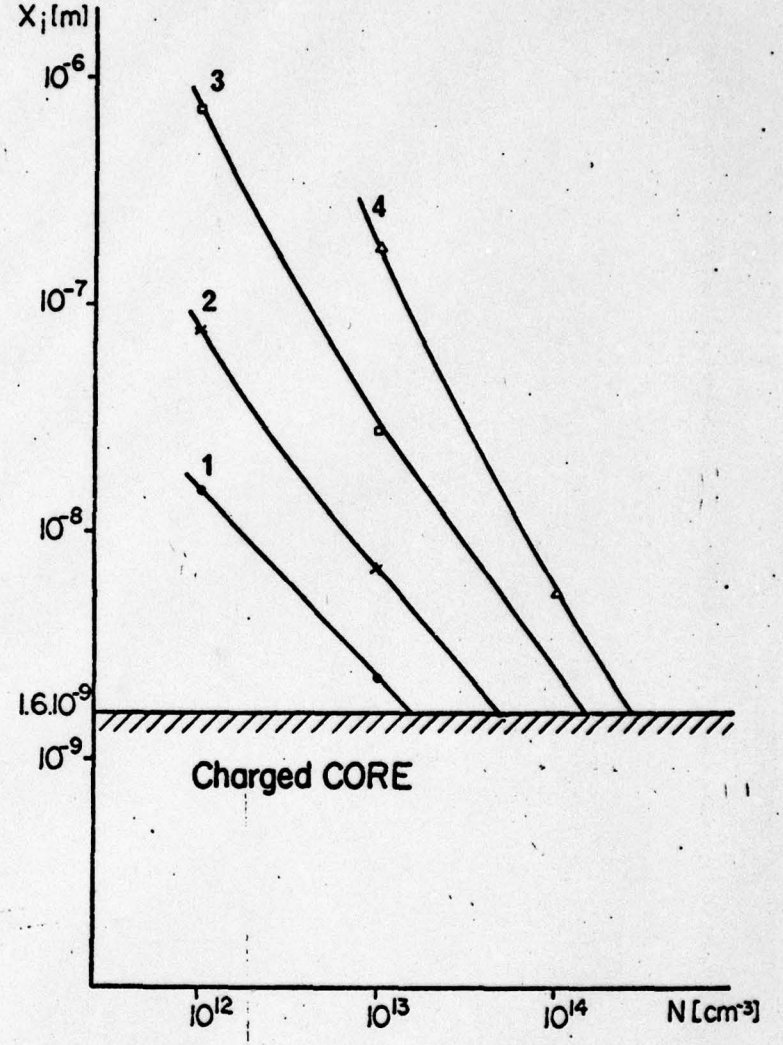
$X_i$[m]
$10^{-6}$
$10^{-7}$
$10^{-8}$
$1.6.10^{-9}$
$10^{-9}$
3
4
2
1
Charged CORE
$10^{12}$
$10^{13}$
$10^{14}$
N[cm$^{-3}$]

Fig 5

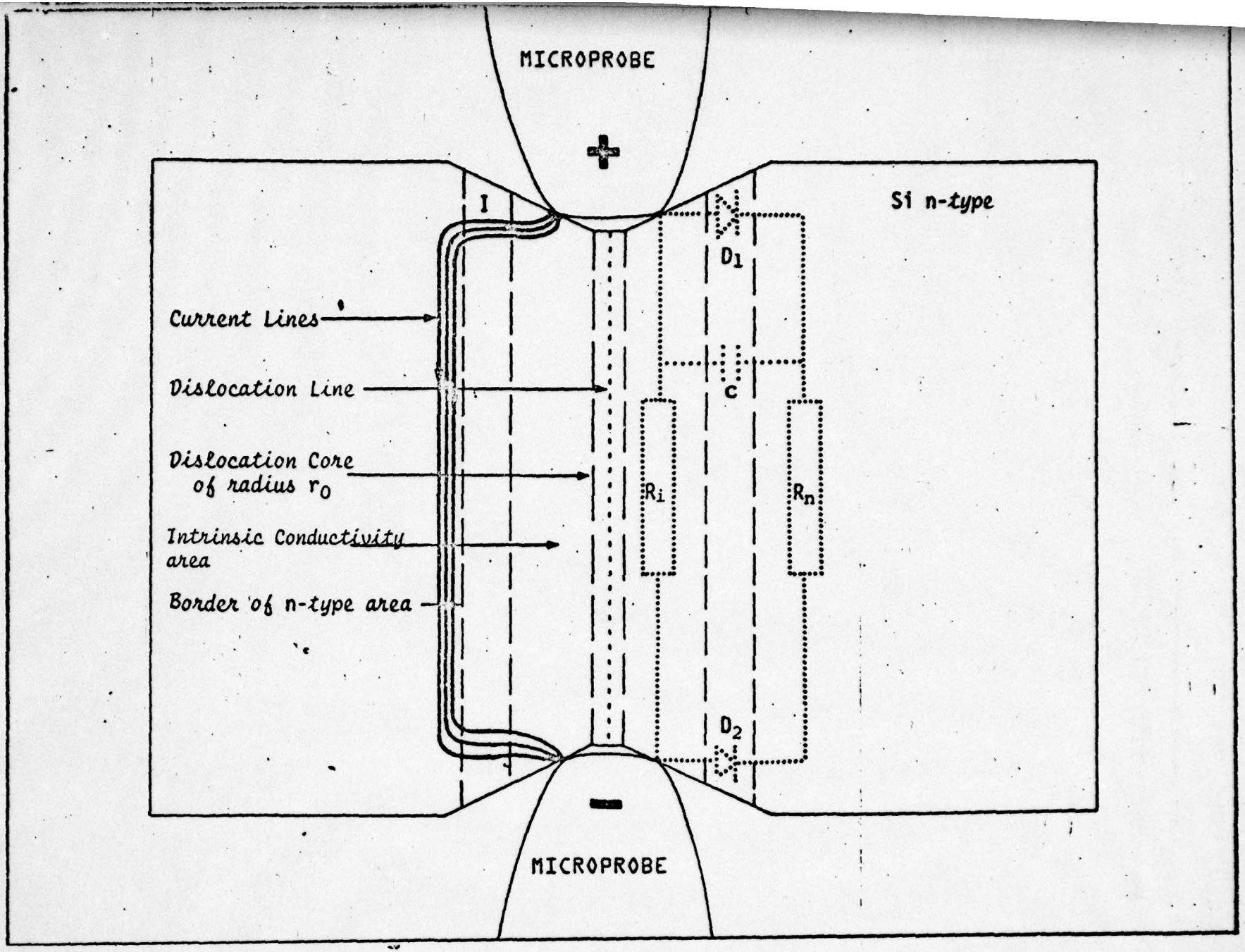
MICROPROBE
+
I
Si n-type
D1
C
Current Lines
Dislocation Line
Dislocation Core
of radius r0
Ri
Rn
Intrinsic Conductivity
area
Border of n-type area
D2
−
MICROPROBE

Fig 7

2

# Appendix E

## On the Possibility of Experimental Observation of the Internal Franz-Keldysh Effect at a Single Dislocation in Si and Ge*

S. Mil'shtein

Department of Physics
Ben-Gurion University of the Negev
Beer-Sheva, Israel

**Abstract**

The electrical field due to different types of single sidelocations in Si and Ge is computed. The possibility of observing the Internal Franz-Keldysh Effects (IFKE) at single dislocations in a wide temperature range is considered. Conditions of such an experiment are discussed.

Submitted to Nuovo Cimento

---

* Supported by U.S. Air Force

In works [1,2] the shift of fundamental absorption edge due to the presence of high dislocation density was observed. In work [2] a number of factors have been listed, pointing out the electrical nature of the observed effect. It has been shown that the change of the absorption coefficient has been caused by electron tunneling in the electric field, associated with dislocations.

A theoretical description of the IFKE at the dislocation cluster faces serious difficulties connected with summing the fields from randomly distributed sources with nonuniform density of dislocations.

Correct integrating with respect to a random configuration of sources is a complicated problem by itself. Finally the concurrent presence of different dislocation types in the cluster brings uncertain information on the dislocations effect upon electro-optical absorption in semiconductors.

The purpose of the present work is to carry out a theoretical examination of the possibility in principle to observe IFKE at single edge-type dislocations in crystals with a different density of impurities in a wide range of temperatures. The details of a possible experiment are briefly discussed.

Earlier refined data on the shape of the electric potential connected with a single dislocation were obtained [3]. In the region near the dislocation line the potential drops slowly according to the logarithmic law. In the more distant region an exponential decreasing of the potential takes place. When the two representations were joined we received a complete description of the area under study [3]. At least two conditions must be met for realizing the IFKE [4]: the electric strength

must be $E = 10^5 - 10^6 \frac{V}{m}$ ; the field must be fairly homogeneous.

Taking the above into consideration, the most interesting region for examination is that near the dislocation where the electric potential is being described in dimensionless form:[3]

$$\varphi = -\frac{r^2}{4} + r_0^2 \left(\frac{1}{2} - \lambda\right) \ell n\, r + .C \qquad (1)$$

where $r_0$ - is the radius of the dislocation core

$r$ - is the current coordinate,

$\lambda$ - is the surface density of the charge on the cylinder (per unit length)

$C$ - is the integration constant

Using $E = -$ grad $\varphi$ we have calculated that strength of electric field around the individual dislocation depends on the type of dislocation, donor concentration $N_d$ and the temperature in the n-type Si and Ge crystals.

Figure 1 presents 60°-dislocation induced electric field E versus donor concentrations. One can see that the slope of curves increases and the radius r of the anomalous area diminishes approximately two orders of magnitude when donor concentration in Si increases for $10^{11}$ $cm^{-3}$ to $10^{17}$ $cm^{-3}$.

Figure 2 shows the electrical field dependence around 60°-dislocation on the donor concentration in Ge. The increasing of $N_d$ from $10^{13}$ $cm^{-3}$ to $10^{17}$ $cm^{-3}$ decreases r approximately the order of magnitude and the curve's slope increases.

Figure 3 presents the strength of the electrical field E as a

function of temperature. We can see that the absolute value E at any point within the anomalous area increases by factor 2 when the temperature changes from 400°K to 100°K.

The same shape of the curves E(t,r) with very small differences in absolute value of E comparatively to the curves presented on Fig. 3 was found for Ge. Therefore the temperature dependences of E in Ge are not presented in this work.

In accordance with the results, presented in Fig. 1 and Fig. 2 we might expect to define experimentally the IFKE in Si with the donor concentration up to $10^{14}$ $cm^{-3}$. Since with increase in concentration of impurities the electrical field $E > 10^5$ v/m will be only within the area of 0.2μ in diameter, it would appear to be very complicated to perform an optical absorption experiment on such a small area. From the experimental point of view, the Ge crystals with $N_d$ up to $10^{15}$ $cm^{-3}$ are preferable.

One can see that electircal field $E > 10^5$ v/m would exist around 60° dislocation within the cylindrical area of about 2μ in diameter at room temperature. Therefore IFKE can be detected in this local area. The IFKE means an increasing of absorption coefficient α, i.e., what is the same shift of fundamental absorption edge to the lowest energy direction.

Recently [2] we established for heavily dislocated Si phonon assisted electroabsorption. The spectral dependence of $\alpha^{1/2}$ showed that absorption process had been accompanied by the emission and absorption of optical phonon $h\omega = 0.06$ eV. If one knew the strength of the internal electrical

field, the IFKE could be easily treated, and $\alpha$ and its shift $\Delta\alpha$ could be defined. In the case of indirect transitions [4]:

$$\alpha = \frac{3}{16} K \left[(\hbar^2 E)^2/2\mu\right]^{2/3} \xi^2 H(\xi) \quad . \tag{2}$$

and

$$\Delta\alpha = K\left[\frac{(\hbar eE)^2}{2\mu}\right]^{2/3} \left\{ \int_{-T}^{\infty} (Z+\xi)^{3/2} / Ai(Z) /^2 dz - \frac{3}{16} \xi^2 H(\xi) \right\} \tag{3}$$

where $e$ - the electron charge, $\mu$ - the reduced mass, $Ai(Z)$ the Airy function and $H(\xi)$ the Heavyside unit function, $K$ - the coefficient of proportionality

$$\xi = [2\mu/(heE)^2]^{1/3} (\hbar\omega - Eg - \hbar\omega) \quad \text{and}$$

$$Z = [2/(heE)^2]^{1/3} [Eg - \hbar\omega + \hbar\bar{\omega}) + h^2p^2/2\mu) \quad .$$

If photon energy $h\omega$ is smaller than the energy gap of material $Eg$, or more precisely if $\hbar\omega < Eg - \hbar\omega$, in this case $H(\xi) = 0$. If $\hbar\omega > Eg - \hbar\bar{\omega}$, than $H(\xi) = 1$. Using Penchina's [5] numerical evaluation of the integral in equation (3) we could easily obtain $\Delta\alpha$ in the case of electron tunneling in the electrical field due to single dislocation.

Expecting electro-optical effects caused by the single edge-type dislocation one must interpret results carefully because of the presence of a strong deformation field around the dislocation line. It must also be pointed out that the existence of deep dislocation centers might result the optical transition [6] in the case when $\hbar\omega < Eg$, which would complicate the interpretation.

In conclusion we shall permit ourselves to make some recommendations concerning the hypothetical experiment. The difficulties of measuring electro-optic effects are usually associated with the dimensions of the part of the crystal exposed to light, since the sensitivity of micro-photometers is generally restricted.

If the electrically anomalous region around the dislocation is small, sensitive photomultipliers, capable of working as photon counters should probably be used. On the other hand the sensitivity of the measuring unit can also be increased by using a small-sized and focused high energy laser beam. But using a laser source will give rise to local overheating of the crystal. Therefore measurements hsould be carried out at low temperatures, which are also suggested by our present calculations (see Fig. 3).

The author would like to express his sincere thanks to Dr. A. Senderichin and Mrs. T. Waksman for their assistance in computation. The author gratefully acknowledges the support of the Air Force Office of Scientific Research and EOARD who sponsored this work under grant AFOS-78-3526.

## References

1. H. Lipson, E. Burstein and P. Smith, Phys. Rev. 99, 444 (1955).

2. S. Mil'shtein, B. Yacobi, Phys. Lett. 54A, 6, 465 (1975).

3. S. Mil'shtein, A. Senderichin, submitted.

4. M. Chester, L. Fritshe, Phys. Rev. 139, 2A, 518 (1965).

5. C. Penchina, Phys. Rev. 138, 3A, 924 (1964).

6. J. Dow, D. Smith, and F. Lederman, Phys. Rev. B 8, 10, 4612 (973).

Figure Captions

Fig. 1. Strength of electrical field around 60°-dislocation versus the distance from the "core" for various donor concentration in Si. 1) $10^{11}$ $cm^{-3}$; 2) $10^{12}$ $cm^{-3}$; 3) $10^{13}$ $cm^{-3}$; 4) $10^{14}$ $cm^{-3}$, 5) $10^{15}$ $cm^{-3}$; 6) $10^{16}$ $cm^{-3}$; 7) $10^{17}$ $cm^{-3}$.

Fig. 2. Strength of electrical field around 60°-dislocation versus the distance from the "core" for various donor concentration in Ge 1) $10^{13}$ $cm^{-3}$; 2) $10^{14}$ $cm^{-3}$; 3) $10^{15}$ $cm^{-3}$; 4) $10^{16}$ $cm^{-3}$; 5) $10^{17}$ $cm^{-3}$.

Fig. 3. Strength of electrical field around 60°-dislocation versus the distance from the "core" for various temperatures in Si. 1) T = 400°K; 2) T = 300°K; 3) T = 200°K; 4) T = 100°K.

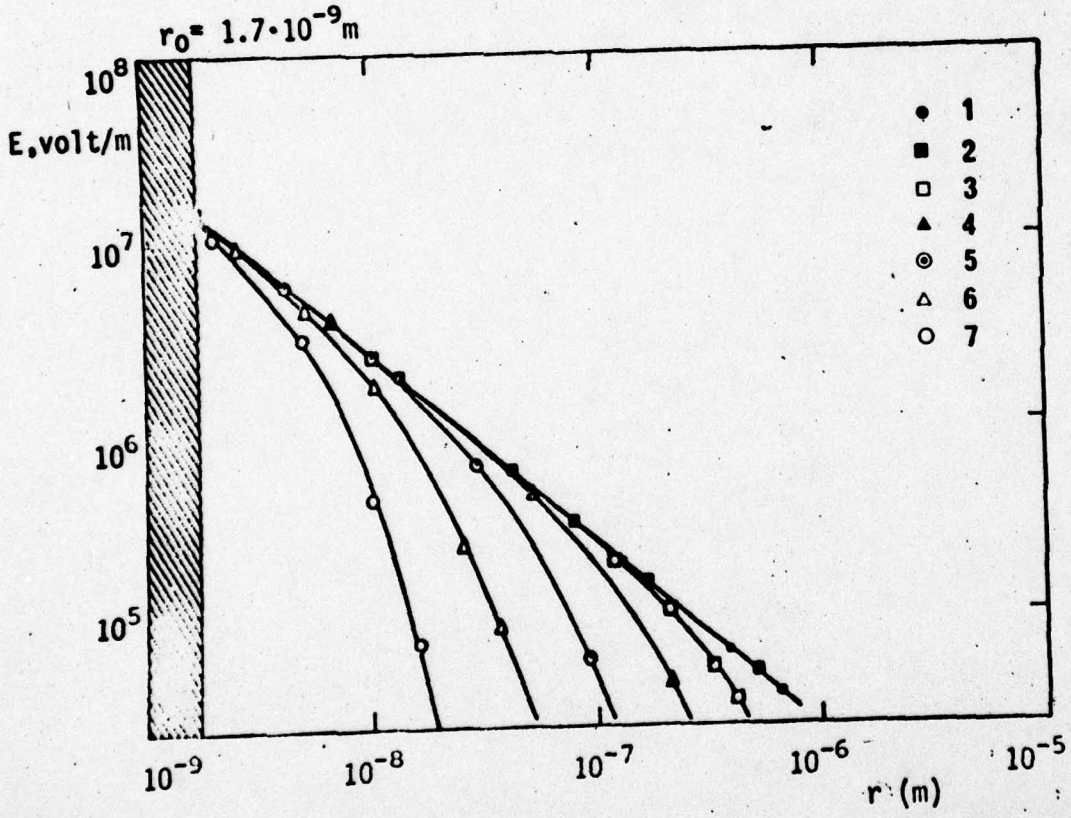
$r_0 = 1.7 \cdot 10^{-9}$ m
$10^8$
E, volt/m
$10^7$
$10^6$
$10^5$
$10^{-9}$
$10^{-8}$
$10^{-7}$
$10^{-6}$
$10^{-5}$
r (m)
1
2
3
4
5
6
7

Fig 1

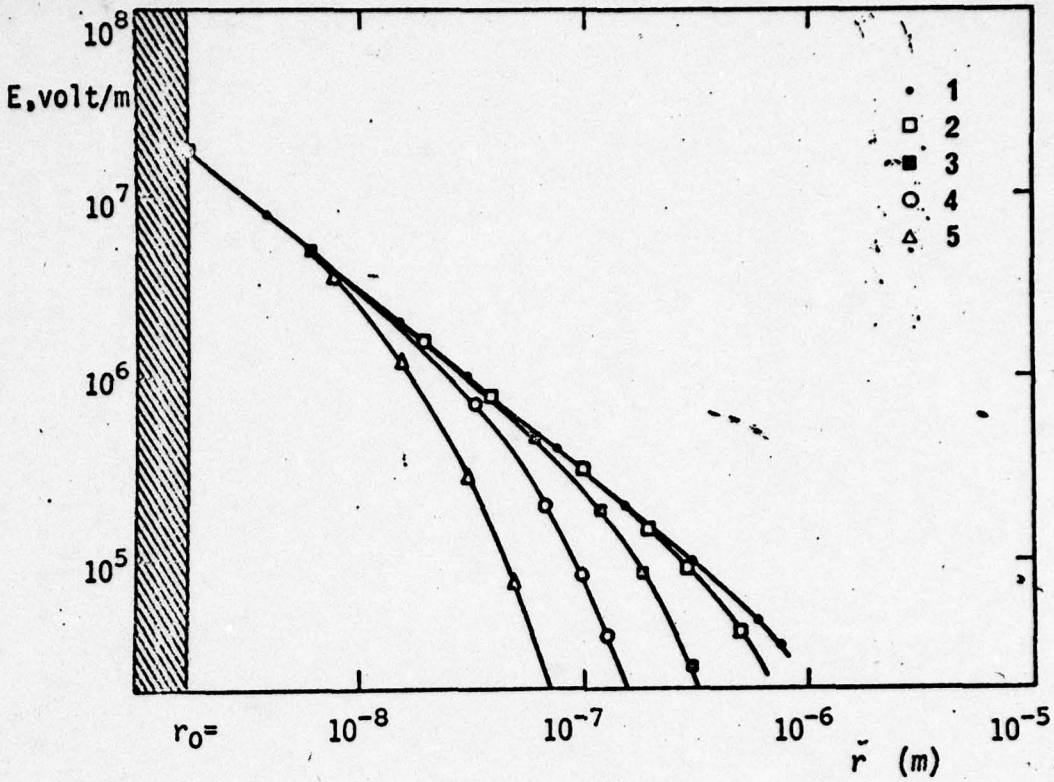


Fig 2

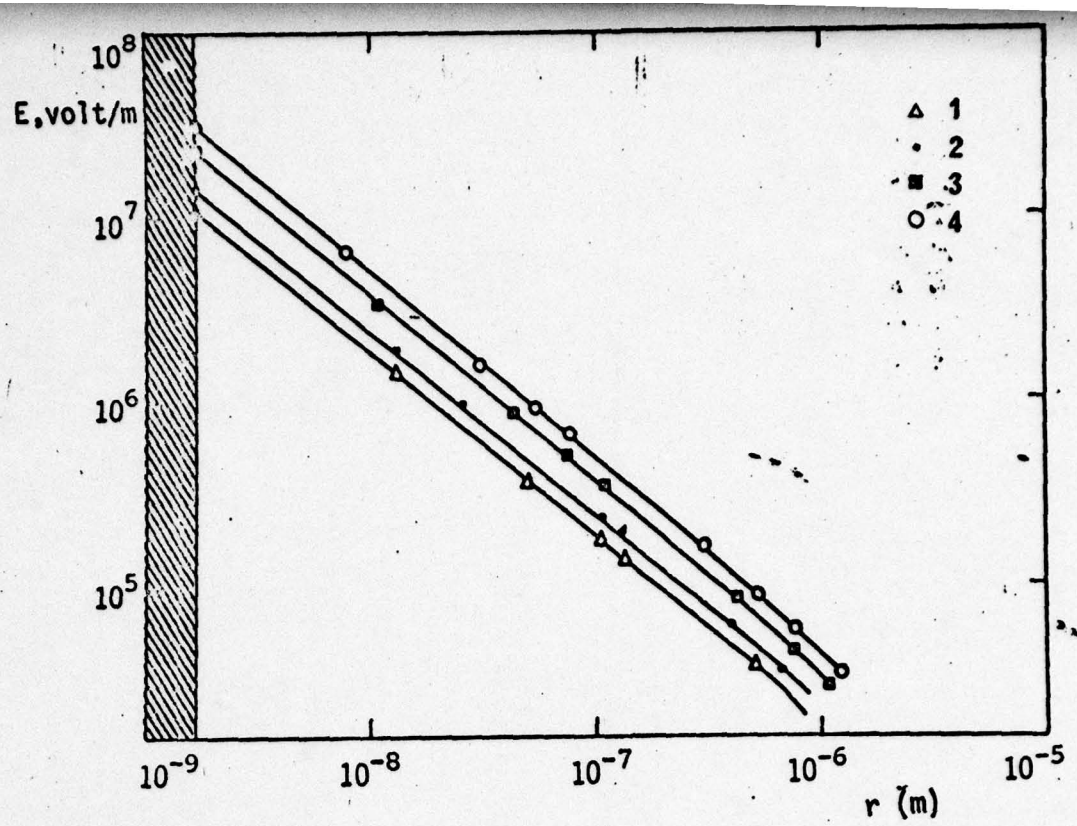


Fig 3.

Appendix F

# ELECTRIC POTENTIALS IN PLASTICALLY DEFORMED Si AND Ge*

S. Kh. Mil'shtein and A.M. Senderikhin

Department of Physics, Faculty of Natural Sciences,
Ben-Gurion University, Beer-Sheva, Israel

## Abstract

The existence of the dislocation electrical barrier (DEB) in plastically deformed semiconductors in wide temperature range is considered. The model of the dislocation p-n junction is used to determine the height of the DEB. The position and width of the energy band due to dislocation is analysed by the aid of the electric neutrality equation. The DEB application problems are briefly discussed.

Submitted to J. Appl. Phys

*Supported by U.S. Air Force

## Introduction

The previously observed diode effect at high density dislocation clusters ($N_{disl} \approx 10^{10} - 10^{11}$ cm$^{-2}$),[1-2] has made it possible to obtain a principally new type of p-n junction in semiconductors, one based on electron-dislocation interaction.[3-4]

The diode effect at dislocations consists of the emergence of p-conductivity in heavily dislocated n-type materials, as a result of the dislocation acceptor action, while the passage of current leads to rectification at the interface of normal and dislocation parts of the crystals.

It has been found that the introduction of the dislocations into the semiconductor crystal results in the emergence of definite energy bands in the gap.[5-7] Hence it is of interest to determine the effect of various crystal parameters and temperature on the height of the dislocation electric barrier (DEB), which may give an additional information about the dislocation-induced energy bands. A study of the dependence of the potential's height on the concentration of free carriers and temperature is also significant for applications.

The purpose of this paper is the theoretical calculation of the DEB dependence on the position of the dislocation energy band and also on the parameters of semiconductor crystals and temperature. To this end the electric neutrality equation has been used to analyse DEB in n-type Si and Ge over a wide temperature range.

## Theory

A model of emergence of a potential barrier in a semiconductor becoming electrically inhomogeneous after plastic deformation has been proposed.[1] According to this model the plastic deformation of covalent crystals introduces a large number of edge-type dislocations, whose broken bonds act as acceptor centers. In computing the p-n junction at dislocations one of the present authors,[8] as also Yeremenko and others[2] who studied the temperature dependences of the electric conductivity of plastically deformed Si, have revealed dislocation energy levels situated above the valency band at distances of 0.39 eV and 0.40 eV, respectively. As a result of overcompensation these acceptor centers create hole conductivity at the dislocation part of the crystal. Thus, the bend of the bands at the interface of the crystal's n- and p-parts is the result of the presence of dislocation-type acceptor centers.

The quantitative and qualitative difference between dislocation acceptors and ordinary chemical impurities makes the dislocation problem an especially complicated one. Let us consider some differences between dislocation acceptors and ordinary chemical impurities. When the latter are introduced into Si and Ge, their solubility is a limiting factor, but the ratio between donors and acceptors can still be changed at will. This does not apply to dislocations. The crystal lattice structure restricts the dislocation density to $10^{10}$ - $10^{11}$ $cm^{-2}$, which is equivalent to $10^{16}$ - $10^{17}$ of broken bonds per cubic cm of the deformed crystal. Since not all dislocations possess an edge component, it will be reasonable to accept $10^{16}$ $cm^{-3}$ as the upper limit of the dislocation acceptors. Naturally,

with a concentration of chemical donor in excess of $10^{16}$ $cm^{-3}$ there will be no overcompensation and, hence, also no electric potential barrier.

An even more important difference between chemical impurities and dislocations can be found. In the case of chemical impurities the emergence of energy bands is typical of considerably large concentrations (of the order of $10^{18}$ $cm^{-3}$). However, a single dislocation forms energy bands. Many authors[9-11] report the presence of one-dimensional G-bands in the upper and lower parts of the forbidden band, as well as one-dimensional secondary band induced by the splitting of the levels from the edges of the valence and conduction bands due to the action of the deformation potential.

The filling of the primary bands[12] is determined by the position of the Fermi level and temperature. However, the main factor limiting the filling of one-dimensional bands is the Coulomb interaction of two neighbouring dangling electrons, which will lead to special statistics for the description of the filling of one-dimensional bands in the proximity of a "harmonic oscillator", "minimum energy", etc.[13]

In the case of high dislocation density we will have uniformly distributed dislocation acceptor centers. The framework of the proposed model takes only the lower G-band or the single acceptor level into account. The upper G-band will contribute to the electric neutrality equation only if it is transversed by the Fermi level. The role of this band will be discussed in greater detail below. For

high dislocation densities the overlapping of electric and deformation potentials will be so strong that the top of the valence and the bottom of the conduction bands must become shallow corrugated surfaces. This allows us not to consider the secondary bands.

As mentioned above, two parts of the crystal are considered: the undeformed, n-type conductivity part and the zone with a high dislocation density and hole conductivity. The problem is practically reduced to finding the Fermi levels in both parts. The difference in the position of the Fermi levels results in the bending of the bands, i.e., in the emergence of an electrical potential barrier.

The electric neutrality equation for the crystal is[14]

$$n + N_a^- - p - N_d^+ = 0 \tag{1}$$

where $N_d^+$ and $N_a^-$ are respectively the densities of the ionized donors and acceptors, and $n$ and $p$ are the free electron and hole concentrations.

All the quantities in equation (1) are connected with the position of the Fermi level and depend on temperature according to the Boltzman law:

$$n = N_c \cdot \exp[(E_f - E_c)/kT] \tag{2}$$

$$p = N_v \cdot \exp[-(E_f - E_v)/kT] \tag{3}$$

$$N_d^+ = N_d \cdot \frac{1}{1 + 2 \cdot \exp[(E_f - E_d)/kT]} \tag{4}$$

$$N_a^- = N_a \frac{1}{1 + \frac{1}{2} \exp[(E_a - E_f)/kT]} \tag{5}$$

where all the designations are commonly accepted ones.

By introducing (2), (3), (4) and (5) into equation 1 and using dimensionless parameters

$$\frac{N_d}{N_c} = A; \quad \frac{N_a}{N_c} = B; \quad \frac{N_v}{N_c} = C$$

$$\frac{E_c - E_d}{kT} = a, \quad \frac{E_c - E_a}{kT} = b, \quad \frac{E_c - E_v}{kT} = c, \quad \frac{E_f - E_c}{kT} = j \tag{6}$$

we obtain

$$e^j + B \cdot \frac{1}{1 + \frac{1}{2}\exp[-(j + b)]} - C \exp[-(j + c)] - A \cdot \frac{1}{1 + 2\exp(j + a)} = 0 \tag{7}$$

Resolving equation (7) separately for the part of the crystal containing dislocations and dislocation -free one, we obtain the position of the Fermi levels in the indicated parts, i.e., the roots $j_1$ and $j_2$. For the dislocation-free part of the crystal the second term of equation (7) is zero.

A simple expression enables us to obtain the height of the potential barrier

$$\Delta\varphi = kT \cdot (j_2 - j_1) . \tag{8}$$

The computations take into account the temperature dependent changes in the density of states and in the width of the forbidden band.

Equation (7) is stated in the event when a single dislocation acceptor level was taken into account. For the case of a dislocation band, the second term of equation (7) has to be slightly modified. We assume that the total number of acceptor states has remained unchanged and that these states are uniformly distributed over the dislocation band. It seems rational to consider the dislocation acceptor band with levels situated at a distance not less than kT. Then the second term of equation (7) is replaced by the sum:

$$e^{j} + \sum_{1}^{m} \frac{1}{n} B_m \frac{1}{1 + \frac{1}{2}\exp[-(j + bm)]} - C \cdot \exp[-(j + c)] - A \cdot \frac{1}{1 + 2\exp(j + a)} = 0 \qquad (9)$$

where $m$ is an integral number of levels in the $G$ dislocation band.

## Results

Equation (9) was used to compute the height of the potential barrier, connected with the dislocation cluster, in n-type Si and Ge for different initial concentration of donor impurities at temperatures ranging from -200° to +200°C. The computation was made when the dislocations were ascribed a single acceptor level and where there was an empty dislocation band of an approximate width of 0.2 eV.

Figure 1 shows the dependence of the DEB on the concentration of the

initial donor impurities in Si at room temperature. The density of the acceptor states Na = $10^{16}$ $cm^{-3}$. We assume a single level $E_a$ = 0.39 eV and $E_a$ = 0.18 eV for Si and Ge, respectively. The choice of these energies is justified by numerous experimental data reported in the literature.[15-18]

Figure 1 shows that the height of the potential barrier in Si increases almost linearly until it reaches a donor concentration of $N_d = 2 \cdot 10^{15}$ $cm^{-3}$, and then rapidly drops to 0.1 eV at $N_d = 5 \cdot 10^{16}$ $cm^{-3}$. The same is observed in Ge, though the drop of the potential is smoother.

Figure 2 illustrates the temperature dependence of the DEB for Si, where there is a single level $E_a$ = 0.39 eV. With rising temperature the potential barrier decreases for donor concentration up to $10^{15}$ $cm^{-3}$ from 0.74 eV to approximately 0.35 eV. Even for $N_d = 10^{16}$ $cm^{-3}$ the potential is still substantial, i.e., of the order of 0.2 eV at +200°C, and changes smoothly within the entire temperature range. The shape of the potentials for $N_d = 10^{17}$ $cm^{-3}$ is not indicated because it remains below 0.005 eV within the entire temperature range.

Figure 3 shows the temperature dependence of the DEB for Ge with a single level $E_a$ = 0.18 eV for donor concentrations of up to $10^{15}$ $cm^{-3}$. For $N_d = 10^{16}$ $cm^{-3}$. The potential changes more smoothly, than in a case of Si.

Figure 4 shows the dependence of the DEB connected with dislocations in Si and Ge for various initial donor impurities concentrations. An empty dislocation acceptor band of 0.39-0.2 eV is assumed for Si and of 0.18-0.09 eV for Ge.

Figure 4 shows the potential rising up to 0.67 eV at temperature T = 0°C, which is higher than the potential calculated when the single level is assumed (see Fig. 2). In Si for the donor concentrations more than $10^{15}$ $cm^{-3}$ the DEB sharply drops. In Ge the height of the DEB reaches 0.3 eV at T = 0°C.

Figure 5 illustrates the temperature dependence of the dislocation potential in Si, assuming the presence of a band at 0.39-0.2 eV above the top of the valence band. It shows a steep increase in the absolute value of the potential barrier as compared with Fig. 2. It reaches 0.5-0.6 eV even at room temperature. The same is observed for Ge in the presence of a dislocation band at 0.18-0.09 eV (see Fig. 6). The absolute values of the potentials are considerably higher than they are when a single level is taken into account (see Fig. 3).

Discussion

1. In plastically deformed n-type Si, when a single acceptor level at $E_a$ = 0.39 eV is taken into account, there must be a DEB, whose height changes from 0.739 eV to 0.176 eV with the rise of temperature from -200°C to +200°C. The current computations may be compared with very few experiments performed on Si n-type. Our calculations show the DEB of about o.4 eV for deformed silicon n-type with $N_d = 10^{13}$ $cm^{-3}$ at room temperature and the measurements performed by S. Mil'shtein [8] on identical crystals gave 0,32 eV. An indirect confirmation of our calculations comes from the work of Eremenko et al. [2], who investigated the I-V characteristics of dislocation p-n junctions and measured their thermoelectric properties. These measurements demonstrated the dislocation diode effect, i.e., the DEB existence in Si with donor concentration from $10^{11}$ $cm^{-3}$ up to $10^{16}$ $cm^{-3}$ in the temperature range from -200°C to +100°C.

At higher temperatures the rectification disappears which is caused by the decreasing of the reverse current, however the DEB still exists. The thermoelectrical measurements at $T > 100°C$ show that the p-type conductivity in the dislocation area remains, i.e., the existence of DEB. In Fig. 2, the area marked of within the rectangle includes the theoretical calculations which coincide with the results readed by Eremenko et al. [2].

2. In plastically deformed n-type Ge, when a single acceptor level at $E_a = 0.18$ eV is taken into account, there must be a potential barrier whose height changes from 0.5 eV to about 0.19 eV with a rise of temperature from -200°C to +100°C, The barrier is still present until the chemical donor concentration reaches a value of about $5 \cdot 10^{15}$ $cm^{-3}$. At temperatures in excess of 100°C the barrier becomes negligible for a donor concentration of $10^{16}$ $cm^{-3}$ (see item 3). Unfortunately the DEB in plastically deformed n-type Ge was not measured and the measurements performed on bicrystals cannot be compared with our calculations for reasons listed below (see item 4).

3. When the presence of an empty dislocation band is taken into account, the potential barrier becomes extremely high. In n-type Si, even at room temperature, the barrier is 0.5-0.6 eV in crystals with an initial donor concentration of $10^{13}$ - $10^{15}$ $cm^{-3}$. This is approximately twice the value measured by us on identical crystals at room temperature.[8]

At low temperatures the barrier almost reaches the magnitude of the forbidden bandwidth (see Fig. 5). We also feel that in n-type Ge, the inclusion of the dislocation band results in an exaggerated magnitude of electric potentials (see Fig. 6).

It should be noted that we have ignored the empty dislocation band near

the bottom of the conduction band. This was done because the Fermi level did not intersect this band in the temperature range considered. As was expected, in conditions of thermodynamic equilibrium this band does not contribute to the basic electric neutrality equations. At the same time, in n-type Ge, with donor concentrations of $10^{16}$ $cm^{-3}$, the Fermi level reaches the upper dislocation band at temperatures of at least -100°C and lower. Therefore that part of curve 4 below -100°C (the dashed line) in Fig. 6 is irrelevant.

Our computations ignore the presence of secondary dislocation bands emerging as a result of the presence of the deformation potential. We have indicated[19] that the shift of the edges of the valence and of the conduction bands at X and L extrema account for no more than $2.7 \cdot 10^{-3}$ eV and $9 \cdot 10^{-3}$ eV, respectively. Hence, the edges of these bands must form finely corrugated surfaces.

4. The exaggerated values for the electric potentials, were obtained, when the empty dislocation bands were taken into account. Potential values approximately as high as those given in Figs. 4, 5 and 6 can be obtained, if it is conjectured that instead of a dislocation band there are single dislocation acceptors: $E_a$ = 0.2 eV for Si and $E_a$ = 0.09 eV for Ge (or even more shallow levels).

Mueller[20] has identified a very high barrier of the order of 0.66 eV in Ge bicrystals at low temperatures and donor concentrations $N_d = 10^{14} - 10^{16}$ $cm^{-3}$. He gives the values of very shallow acceptor states, approximately 0.04 eV. However, the common shortcoming of measurements on bicrystals is that it is impossible to unambiguosly determine

the role played by dislocation acceptor states because an electric barrier may form during the growth of bicrystals as a results of the segration of impurities, the formation of Cottrell atmospheres[21] or the presence of oxygen.[22]

Furthermore, our measurements[8] have shown that the DEB is much lower (see item 1) than the calculated one. Hence an existence of deep lying single acceptor levels or bands due to dislocations seems more reasonable.

5. Our calculations for wide (bandwidth about 0.2 eV) an deeply-lying dislocation band show that at temperatures below -150°C the potential barrier becomes so high that the Fermi level in the non-deformed n-type part of this crystal touched the bottom of the conduction band, and passes through the values of the dislocation band in the p-type part. In this case the voltage-current characteristics must resemble the characteristics of tunnel diodes. However, the tunnelling effect has not been observed by anyone, even though low temperature measurements were made on Ge bicrystals[20,23] and heavily dislocated Si,[2] where the density of dislocation acceptors up to $10^{17}$ $cm^{-3}$ had inidcated.

6. We obtain an exaggerated value of DEB when we start to fill the dislocation band from its bottom (the empty dislocation band). Only assuming the Fermi level displacement in the upper part of the dislocation band, we get the value of DEB which is in agreement with experiment. In terms of Labush-Schröter's model[6] it means that the dislocation band is half-filled from the very beginning. The Fermi level did not lie lower than the middle of the dislocation band which once again emphasizes the acceptor character of the dislocation states. Our calculations show that

Fermi level is pinned to the top of the dislocation band. Such a pinning is usual in overcompensated semiconductors.

Checking our model we calculated the filling factor f in the temperature range from 20°C to -200°C. With decreasing temperature f changed from 0.64 to only 0.66.

In our method we assumed that the dislocation states can be i) empty, ii) occupied by one electron, iii) occupied by two electrons. Therefore f being equal to 0.5 means that the energy states are filled by one electron and only 14% of the broken bonds have the second electron at room temperature. Classical Read theory however deals with much smaller f caused by repulsing Coulomb interaction between the electrons captured along the dislocation line. In the case of very high density of dislocations such an interaction can be neglected because the dangling bonds are uniformly distributed very close to each other and which results in the usual filling mechanism and normal value of f.

The considerations outlined in items 4, 5 and 6 would seem to warrant the following conclusion about dislocation-linked energy levels:

(a) dislocations are connected predominantly with deep states,
(b) the plastic deformation of crystals, probably, leads to the emergence of deep-lying, narrow energy bands, whose width, apparently, does not exceed several hundredths of electronvolt.

The views expressed here are in good agreement with the experimental results of many researchers[24-28] who find the deep single dislocation acceptor levels or narrow bands, even if they contradict those of as many others.[29-31]

7. The proposed method of computing the height of DEB and the conditions of its existence can, apparently, also be applied to p-type Ge and Si. In hole materials, the indicated method will make it possible to compute potential barriers of the $p\text{-}p^+$ type.

We believe that the proposed method is applicable not only to Ge and Si, but also to any plastically deformed semiconductor in which the DEB is of practical interest. Unfortunately, the fact that we did not consider the interaction of dislocations with the point defects and the complicated structure of the dislocation "core", the presence of kinks and jogs etc. is the main drawback to the proposed model. Although it is possible to avoid the side effects after various types of annealing, the proposed method must be considered as the first approach to the problem.

8. The possibility of creating dislocation p-n junctions applicable over a broad range of temperatures has previously been linked exclusively to high resistance materials. The reason for this was that the over-compensation or inversion of the conductivity of n-type semiconductors caused by the emergence of dislocation acceptors was considered possible only in materials with a small number of free electrons. The above computations show that materials of a lower resistance can be used for that purpose as well.

The properties of p-n junctions, of course, are determined not only by the height of DEB. Many other physical and geometrical factors, now being studied in our laboratory may be important as well.

The authors gratefully acknowledge the support of the Air Force Office of Scientific Research and EOARD who sponsored this work under grant AFOS-78-3526. The authors wish to express their gratitude to Mrs. T. Waksman for her help in these computations.

Figure Captions

Fig. 1. DEB dependence on the donor concentration in the case of single dislocation level.

Fig. 2. DEB temperature dependence in Si for the case of single dislocation level and the concentrations: 1-$10^{11}$ $cm^{-3}$, 2-$10^{12}$ $cm^{-3}$, 3-$10^{13}$ $cm^{-3}$, 4-$10^{14}$ $cm^{-3}$, 5-$10^{15}$ $cm^{-3}$, 6-$10^{16}$ $cm^{-3}$.

Fig. 3. DEB temperature dependence in Ge for the case of single dislocation level and the concentrations 1-$10^{13}$ $cm^{-3}$, 2-$10^{14}$ $cm^{-3}$, 3-$10^{15}$ $cm^{-3}$, 4-$10^{16}$ $cm^{-3}$.

Fig. 4. DEB dependence on the donor concentration in the case of dislocation band.

Fig. 5. DEB temperature dependence in Si for the case of dislocation band and the concentrations: 1-$10^{11}$ $cm^{-3}$, 2-$10^{12}$ $cm^{-3}$, 3-$10^{13}$ $cm^{-3}$, 4-$10^{14}$ $cm^{-3}$, 5-$10^{15}$ $cm^{-3}$, 6-$10^{16}$ $cm^{-3}$.

Fig. 6. DEB temperature dependence in Ge for the case of dislocation band and the concentrations: 1-$10^{13}$ $cm^{-3}$, 2-$10^{14}$ $cm^{-3}$, 3-$10^{15}$ $cm^{-3}$, 4-$10^{16}$ $cm^{-3}$.

## References


1. S. Mil'shtein and V. Nikitenko, Sov. Phys.-Solid State 16, 346 (1974).
2. V. Eremenko, V. Nikitenko, E. Yakimov, Zh. Exp. Teor. Fiz. 67, 1148-1160 (1974).
3. S. Mil'shtein, Bull. Israel Phys. Soc. 21, 40 (1975).
4. S. Mil'shtein, USA patent No. 4005523 from April 9, 1975, published Feb. 1977.
5. R. Labush, R. Schelter, Phys. Stat. Sol. A 9, 455 (1972).
6. R. Labush, W. Schröter, Lattice Defects in Semiconductors, Conference Series, No. 23, The Institute of Physics, London (1975), p. 56-72.
7. R. Jones, Phil. Mag. 35, 1, 57 (1977).
8. S. Mil'shtein, J. Appl. Phys. 46, 9, 3894 (1975).
9. V. Bonch-Bruevich and V. Glasko, Sov. Phys.-Solid State 3, 26 (1961).
10. D. Mergel and R. Labush, Phys. Stat. Sol. A, 41, 431 (1977).
11. H. Weber, Phys. Stat. Sol. A, 25, 445 (1974).
12. W. Read, Phil. Mag. 45, 775 (1954).
13. W. Bardsly, Progress in Semiconductors, Vol. 4, Wiley, New York (1960), p. 157.
14. E. Spenke, Electronic Semiconductors, New York: McGraw-Hill (1958), p. 307.
15. E. Kamieniecki, Phys. Stat. Sol. A, 4, 257 (1971).
16. A. Fortini, Phys. Stat. Sol. 32, 369 (1969).

17. R. Glaenzer and A. Jordan, Solid-Stat. Electron. 12, 247 (1969).

18. Yu. Osip'yan and S. Shevchenko, Sov. Physics, JETP, 34, 6, 1248 (1972).

19. S. Mil'shtein and B. Yacobi, Phys. Letters 54A, 6, 465 (1975).

20. R. Mueller, J. Appl. Phys. 30, 4, 546 (1959).

21. H. Queiser, Festkorperprobleme II, Vieweg, Braunschweig, 1963, p. 162.

22. A. Seybolt, J. Westbrook, D. Turnbull, Acta Metallurgica, 12, 1456 (1964).

23. Yo. Hamakawa and J. Yamaguchi, Jap. J. Appl. Phys. 1, 6, 334 (1962).

24. R. Jones, Phil. Mag. 36, 3, 677 (1977).

25. W. Barth, K. Elsaesser, W. Güth and E. Kamieniecki, Phys. Stat. Sol. A, 39, 249 (1977).

26. M. Jastrzebska and T. Figielski, Phys. Stat. Sol. 14, 381 (1966).

27. Z. Golacki and T. Figielski, Phys. Stat. Sol. 20, K1 (1967).

28. H. Kos, D. Neubert, Phys. Stat. Sol. A, 44, 259 (1977).

29. A. Cavallini, P. Gondi and A. Castaldini, Phys. Stat. Sol. A, 43, K205 (1977).

30. V. Grazhulis, V. Kveder, V. Mukhina, Phys. Stat. Sol. A, 44, 107 (1977).

31. W. Schröter, Phys. Stat. Sol. 21, 211 (1967).

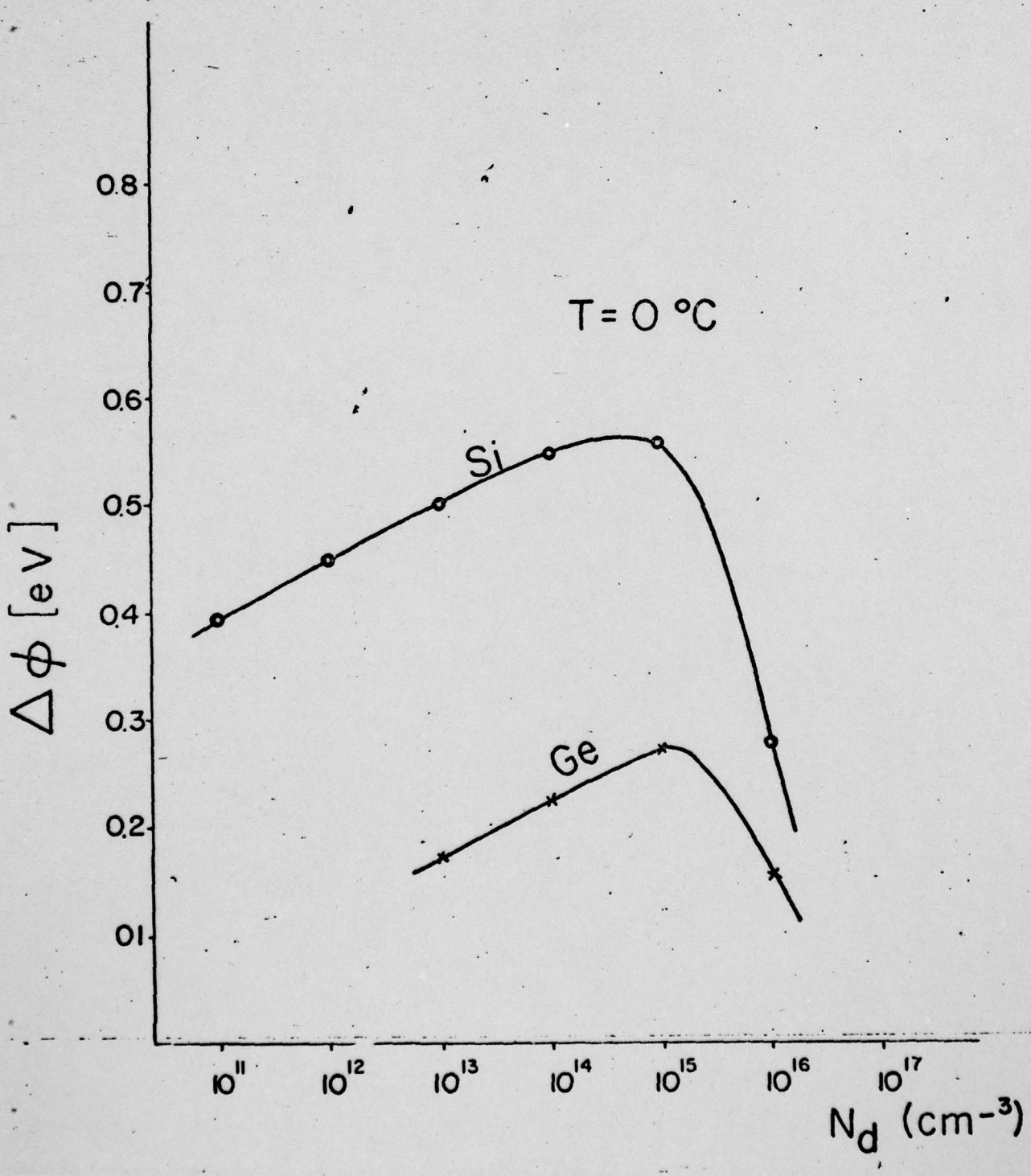
T = 0 °C
Si
Ge
Δφ [eV]
0.8
0.7
0.6
0.5
0.4
0.3
0.2
01
10^11
10^12
10^13
10^14
10^15
10^16
10^17
N_d (cm^-3)

Fig 1

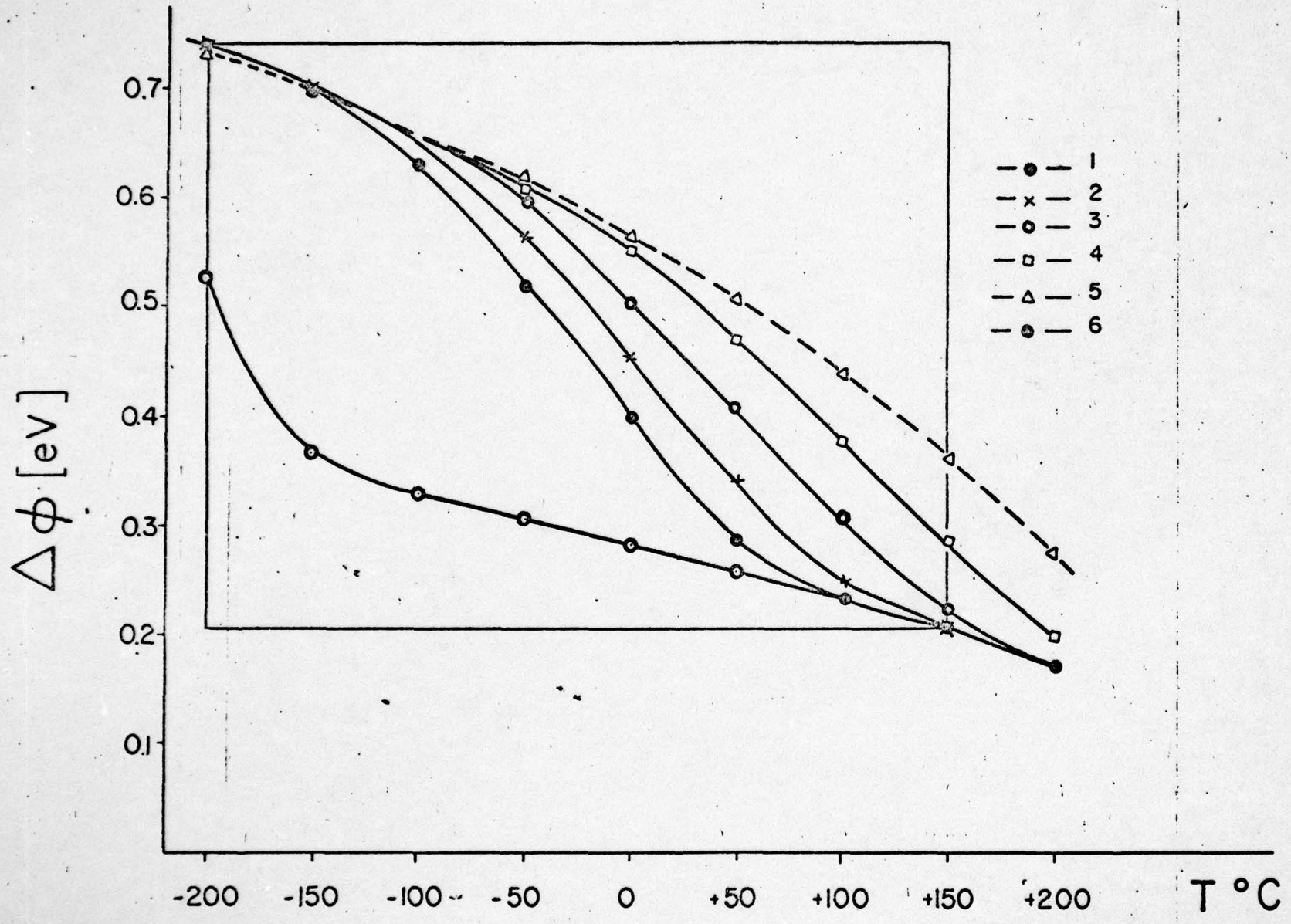


Fig 2

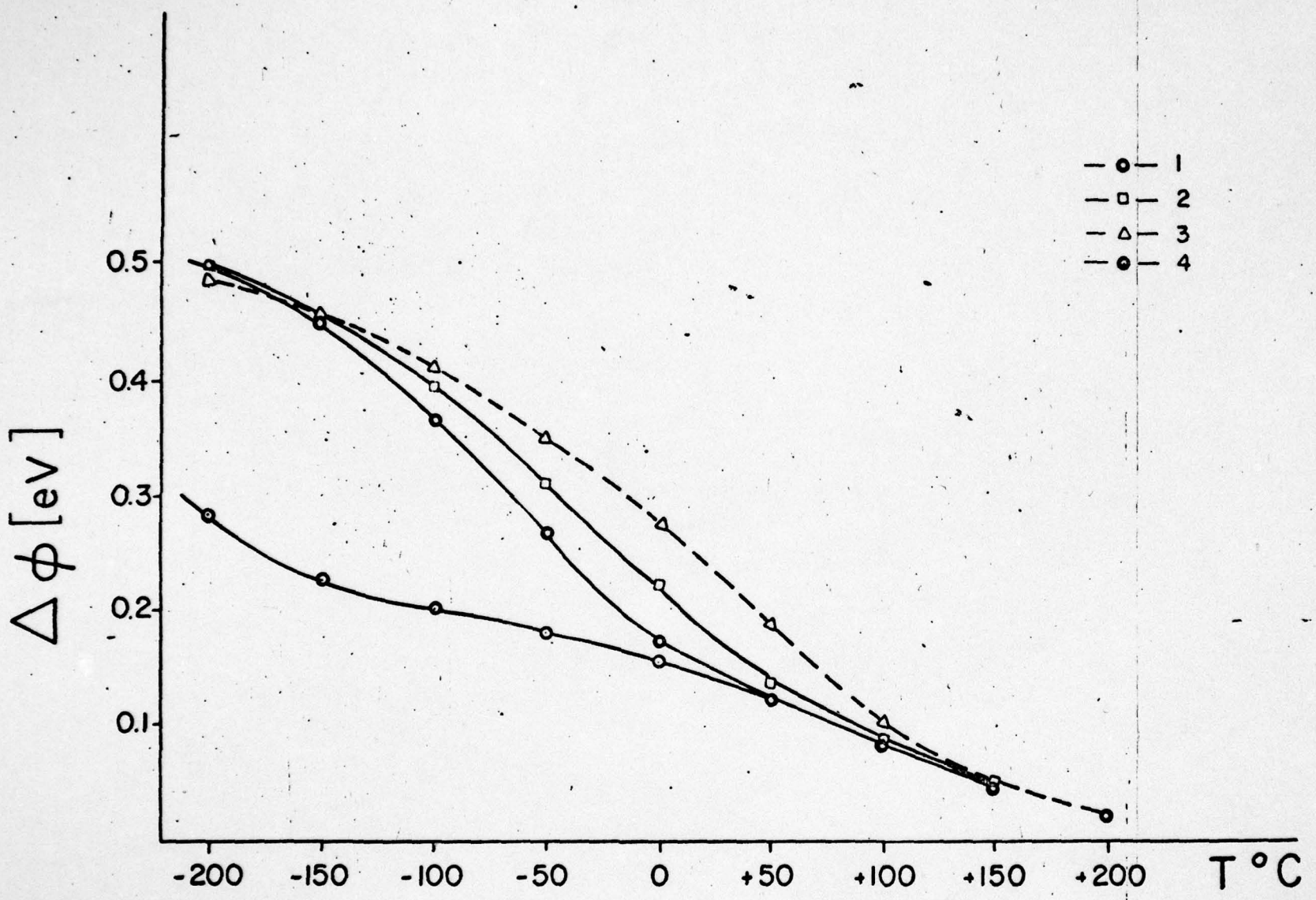


Fig 3

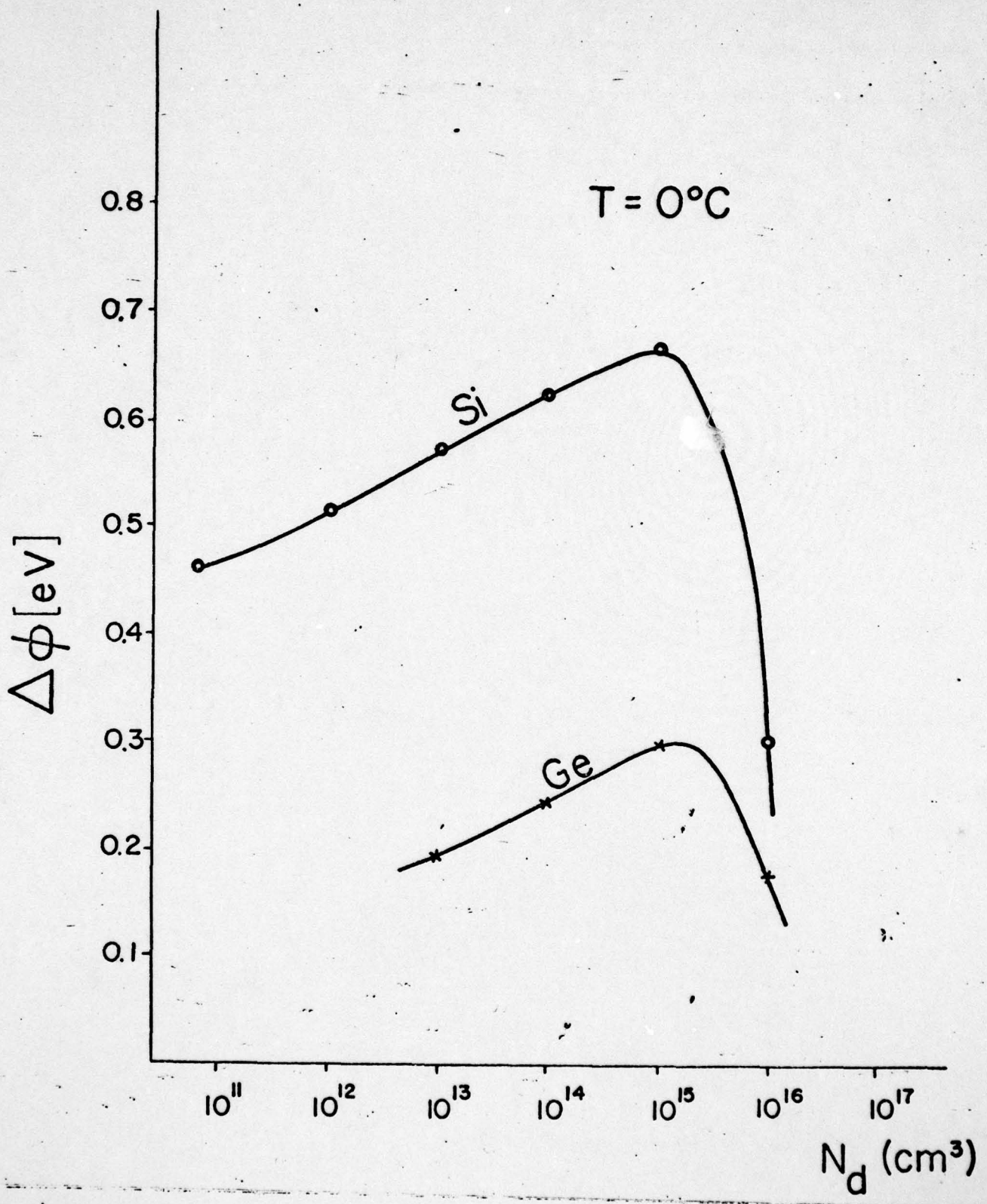
T = 0°C
Si
Ge
Δφ [eV]
0.8
0.7
0.6
0.5
0.4
0.3
0.2
0.1
10^11
10^12
10^13
10^14
10^15
10^16
10^17
N_d (cm^3)

Fig 4

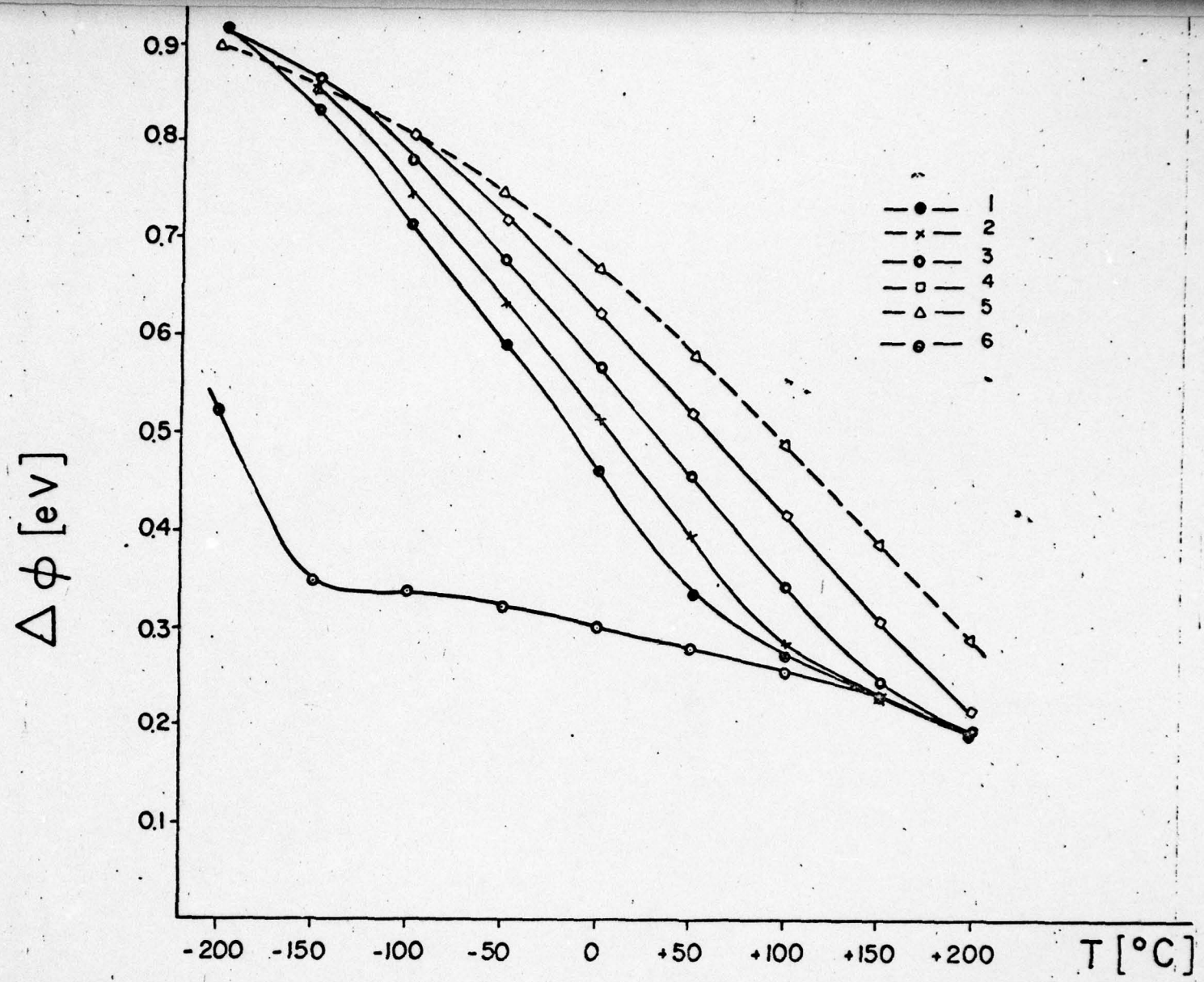
0.9
0.8
0.7
06
0.5
0.4
0.3
0.2
0.1
Δ φ [eV]
-200
-150
-100
-50
0
+50
+100
+150
+200
T [°C]
1
2
3
4
5
6

Fig 5

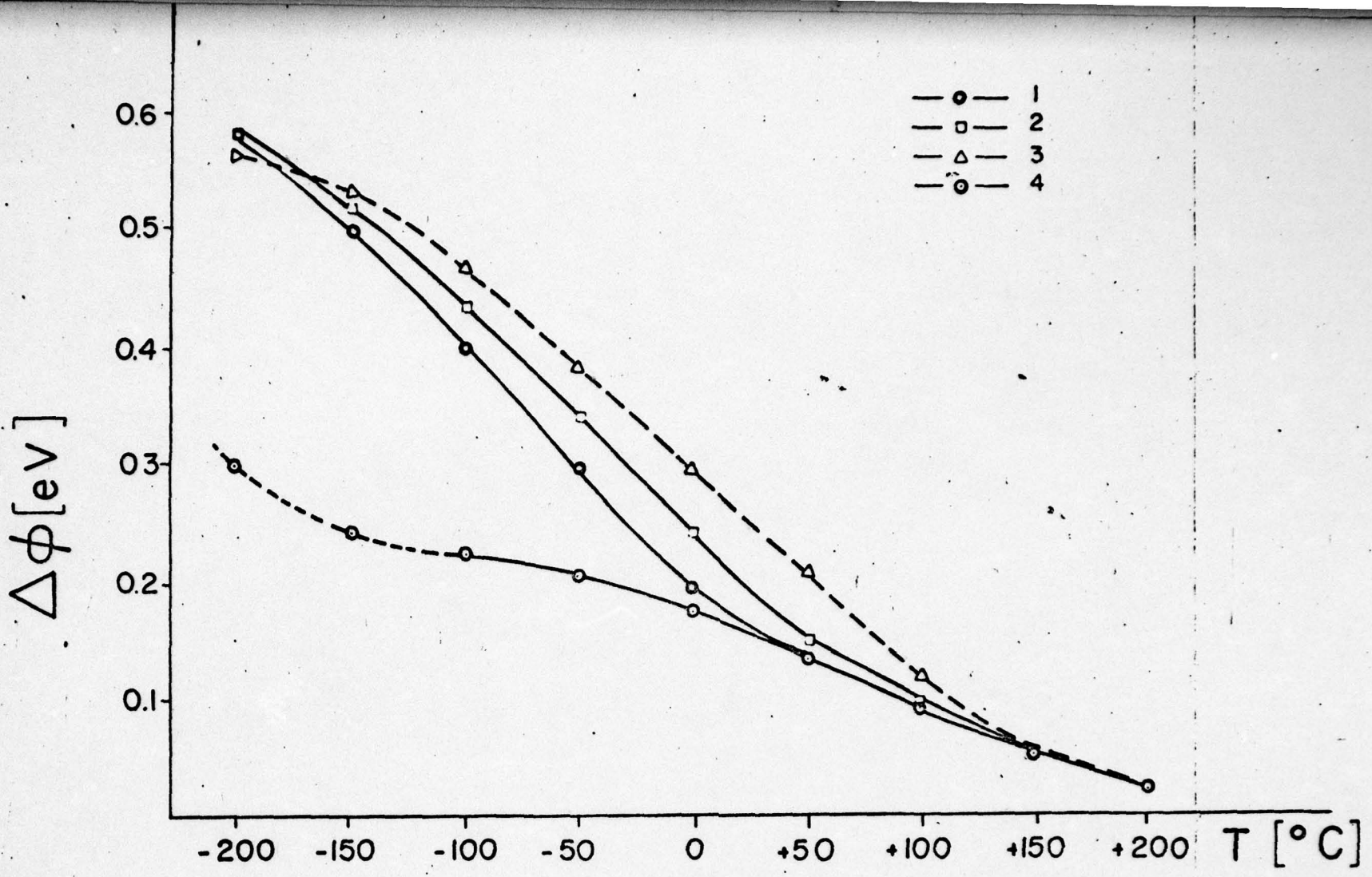


Fig 6

Appendix G

# DIFFERENTIAL PHOTOCONDUCTIVITY GENERATED FROM IMPURITY AND DEFECT STATES IN SEMICONDUCTORS*

S. Mil'shtein A. Senderichin

Department of Physics, Faculty of Natural Sciences,
Ben-Gurion University of the Negev, Beer-Sheva, Israel

The differential method of measurements of the photoconductivity generated from impurity and defect states is considered. It was shown, that in a case of monopolar photoconductivity the new method could yield information on the optical parameters of the materials. Experimental details were discussed.

Submitted to Solid State Communication

AD-A079 592 BEN-GURION UNIV OF THE NEGEV BEERSHEBA (ISRAEL) F/G 20/12
DISLOCATION INFLUENCE ON THE ELECTRICAL AND OPTICAL PROPERTIES --ETC(U)
1979 S MIL'SHTEIN AFOSR-78-3526

UNCLASSIFIED AFOSR-TR-79-1355 NL

2 OF 2
AD A
079592

END
DATE
FILMED
2 — 80
DDC

## 1. Introduction

The main purpose of the differential photoconductivity [DPM] measurements[1] consisted of the elimination of surface effect. We developed this method[1,2] in order to obtain information on light absorption in the material and on some other parameters of this material such as diffusion length, quantum yield etc.

We have recently derived equation[1,2] which describe the intrinsic photoconductivity. Taking into account band-to-band electron transitions we obtained the differential equations whose solutions serve as the exact definition for the experimental measurements. In the case of extrinsic doped semiconductors the light excitation of the impurity states as well as different kinds of recombination processes give rise to its own specificity. The DPM application for semiconductors, containing different energy levels (like impurities, dislocations, deep states) will be considered in this paper.

## 2. Theory

In the case of illuminated thick doped semiconductor crystals the absorption coefficient $\alpha$ is not a constant quantity, but changes with depth in the crystal. Variations $\alpha$ are determined by the ratio between the numbers of incident photons and the number of impurity states. Only with high illumination all the impurity levels will be excited, and the coefficient $\alpha$ begins to be a constant quantity. Depending on the type of recombination and on the number of major carriers, the photoconductivity may be monopolar or bipolar. Let us consider the case of monopolar photoconductivity in n-type semiconductors containing deep impurity levels, dislocations, radiation defects and so on. The diagram of virtual transitions of electrons between deep levels and conductivity and valence bands respectively is shown in fig.1.

1. The number of electron transitions $[\frac{1}{cm^3 sec}]$ to the conduction band from the impurity centres excited by light will equal ($\beta q m I$) where:
   - I - is the intensity of light,
   - $\beta$ - quantum yield,
   - q - cross section of the deep center,
   - m - number of deep states.
2. The intensity of thermal generation will be ($\gamma_n \cdot m \cdot N_{cm}$), where
   - $N_{cm}$ - equilibrium electron density by reducing Fermi-level to traps,

$\gamma_n$ - cross section of electron.

3. The recombination of electrons on free deep levels (traps) i.e. intensity of reverse transitions of electrons from the conductivity band to deep levels.

The following designations are used here:

$I[\frac{1}{cm^2 sec}]$ - the intensity of light,

M, m - concentration of impurity states and concentration of levels, occupied by electrons respectively,

$\gamma_n, \gamma_p$ - cross sections of electron and hole respectively,

$N_{CV}$ - effective density of electron states in the conduction band reduced to impurity levels:

$$N_{CM} = N_c \cdot \exp(-\frac{\Delta \varepsilon_m}{KT})$$

$P_{VM}$ - effective density of hole states in the valence band reduced to impurity levels:

$$P_{VM} = P_v \cdot \exp(-\frac{\Delta \varepsilon_g + \Delta \varepsilon_m}{KT})$$

$\beta$ - quantum yield, $\Delta\varepsilon_m$-energy of deep states, $\Delta\varepsilon_g$-energy gap.

Let us consider the monopolar conductivity when transitions 4 and 5 are neglected.

For stationary photoconductivity

$$divj = divj_n + divj_p \equiv 0 \qquad (1)$$

and for monopolar photoconductivity:

$$divj_n = 0 \qquad (2)$$

In one-dimensional case:

$$div_x j_n = \frac{d(Jx/-e)}{dx} = \beta qmI + \gamma^m N_{CM} - \gamma(M-m)n \qquad (3)$$

for the sake of simplicity $\gamma$ is written without index "n".

It is clear for this case:

$$\Delta m = -\Delta n$$
$$m = m_0 + \Delta m$$
$$n = n_0 + \Delta n \qquad (4)$$

where:

$m_0$ - the equilibrium concentration of electrons on impurity centres and

$n_0$ - the equilibrium concentration of electrons in the conduction band.

Substituting the set of equations (4) into the equation (3) after some transformations, we obtain:

$$\left(-\frac{1}{e}\right)\frac{d J_x}{dx} = \beta q(m_0-\Delta n)I - \gamma\Delta n(n_0+\Delta n+M-m_0+N_{CM}) +$$

$$+ \gamma m_0 N_{CM} - \gamma M n_0 + \gamma m_0 n_0 . \qquad (5)$$

But the last term in equation (5) is equal to zero due to the equilibrium condition in the dark (I=0): the thermal electron transitions to the conduction band are compensated by the reverse transitions of electrons from the conduction band (recombination through free impurity states).

Taking into account the equation (2) and substituting the following expression:

$$I = I(0)\cdot\exp(-\alpha x) = I(0)\cdot\exp[-q(m_0-\Delta n)]x$$

I(0) - the light intensity on semiconductor surface, we obtain the nonlinear algebraic equation for the excess concentration $\Delta n(x)$:

$$\beta\cdot q\cdot(m_0-\Delta n)\cdot I(0)\cdot\exp[-q(m_0-\Delta n)x] -$$

$$- \gamma\Delta n\cdot(n_0+\Delta n+N_{CM}+M-m_0) = 0 \qquad (6)$$

For the case of weak illumination it is possible set:

$$\Delta n \ll m_0$$

and then this equation (6) becomes the linear one:

$$\beta q m_0 I(0)\cdot\exp(-qm_0 x) - \gamma\cdot\Delta n\cdot(n_0+N_{cm}+M-m_0) = 0 \qquad (7)$$

$$\Delta n = \frac{\beta q m_0 I(0)\cdot\exp(-qm_0 x)}{\gamma(n_0+N_{cm}+M-m_0)} = A\cdot I(0)\cdot\exp(-\alpha x). \qquad (8)$$

where: the constant $A(\gamma, n_0, N_{cm}, M, m_0, \beta, q)$ depends on the parameters of material only.

From the last equation we obtain:

$$\alpha = \frac{\ell n\,\frac{\Delta n(1)}{\Delta n(2)}}{x_2 - x_1} \qquad (9)$$

where $\Delta n(1)$ and $\Delta n(2)$ are the excess concentrations in the two layers, deposed on the depths $x_1$ and $x_2$ respectively.

Equation (9) allows us to obtain the spectral distribution of the absorption coefficient by means of differential photoconductivity measurements. In equation (9) information on the surface parameters (recombination velocity and so on) is lacking. This results from the fact that in the case of monopolar conductivity neighbouring layers of crystal do not influence each other; since the

generation and recombination processes of carriers occured in the same volume. In other words the cloud of generated electrons has no time to diffuse a large distance away because of the small time of the Maxwell relaxation and all generated electrons recombine in the same volume.

Let us consider now bipolar photoconductivity when the light excitation is accompanied by the thermal electron transitions from the valence band to deep levels. As will be shown below unfortunately the formalism elaborated for intrinsic photoconductivity is not applicable to bipolar extrinsic photoconductivity. In the case of intrinsic photoconductivity[2] the recombination term of "the symmetric kind"

$$\tau = \frac{p\Delta n + n\Delta p}{(p+n)\tau} \qquad (10)$$

is included into the continuity equation. The Poisson's equation allowed us to eliminate the field strength E(x) from expressions for electron and hole concentrations. n(x) and p(x) which can be presented in the same form:

$$\frac{\partial n}{\partial t} = \frac{\partial p}{\partial t} = \alpha\beta I - \frac{p \cdot n - p_0 n_0}{\tau_n (p+p_0) + \tau_p (n+n_0)} = 0 \qquad (11)$$

Unfortunately, in the case of bipolar photoconductivity we will have two different equations:

$$\frac{\partial n}{\partial t} = \alpha\beta I - \gamma_n \cdot n(M-m) + \gamma_n m N_{CM}$$

$$\frac{\partial p}{\partial t} = - \gamma_p m p + \gamma_p (M-m) P_{VM} \qquad (12)$$

As a consequence it is impossible to eliminate the generation term $\alpha\beta I$ from the expressions (12) and to obtain a formula like expression (10). The presence of the unknown function E(x) makes it impossible to solve these differential equations in analytical form.

Thus the differential photoconductivity measurements can be applied for crystals with intrinsic photoconductivity or with monopolar extrinsic photoconductivity. Let us estimate the criterion of application of the new photoconductivity measurements for extrinsic photoconductivity crystals.

In fact, this criterion must be the criterion of monopolar photoconductivity

$$\frac{\Delta n}{\Delta p} \gg 1 \qquad (13)$$

It is possible to prove that this condition is equivalent to:

$$\frac{m_0^2}{MP_{VM}} >> 1 \qquad (14)$$

Therefore the monopolar photoconductivity is realized

a) by small $P_{VM}$ (when all centres lie far from the band's edges, since the thermal exchange with these bands leads to the bipolarity,
b) the impurity levels m are almost filled ($\frac{m}{M} \simeq 1$).

The estimations show that in Ge and in Si for deep levels near the centre of the gap the monopolar photoconductivity begins from very small concentrations, $M >> 10^6 cm^{-3}$.

### 3. Discussion

1) We have proposed a method of differential photoconductivity measurements in the intrinsic crystals, which may be used for the case of monopolar extrinsic photoconductivity with deep impurity centres and concentration of $M \gtrsim 10^3 cm^{-3}$. for low levels of illumination. Such measurements allow us to obtain information about photoconductivity and absolute value of absorption coefficient as well. It is also possible to perform the proposed measurements with shallow impurity levels at low temperatures, when thermal generation does not distort the measurements.

2) As follows from equation (10) it is sufficient to carry out the measurements on two and not on three layers as in the case of intrinsic photoconductivity. The experimental measurements may be carried out using our previously proposed method.

3) Unfortunately, this method proposed earlier can not be used in the case of bipolar photoconductivity. The criterion of monopolar photoconductivity, considered above, may be presented in different forms: as relationships

$$\frac{m_0^2}{MP_{VM}} = \frac{n_0^2}{n_i^2}\alpha = p_0^2\alpha >> 1. \qquad (15)$$

The authors gratefully acknowledge the support of the Air Force Office of Scientific Research and EOARD who sponsored this work under grant AFOS-78-3526.

Figure Captions

Fig.1. Scheme of the electron transitions

1. - optical generation from the deep states.
2. - thermal generation from the deep states.
3. - recombination of electrons at free deep levels.
4. - thermal generation from the valence band to the deep levels.
5. - electron transitions from the deep levels to the valence band.

* Supported by US Air Force

REFERENCES

1. MIL'SHTEIN, S., and SENDERICHIN, A., Bull Israel Phys. Soc., 25, 20. 1979.

2. MIL'HSTEIN, S., and SENDERICHIN, A., Phys. Rev. (in press).

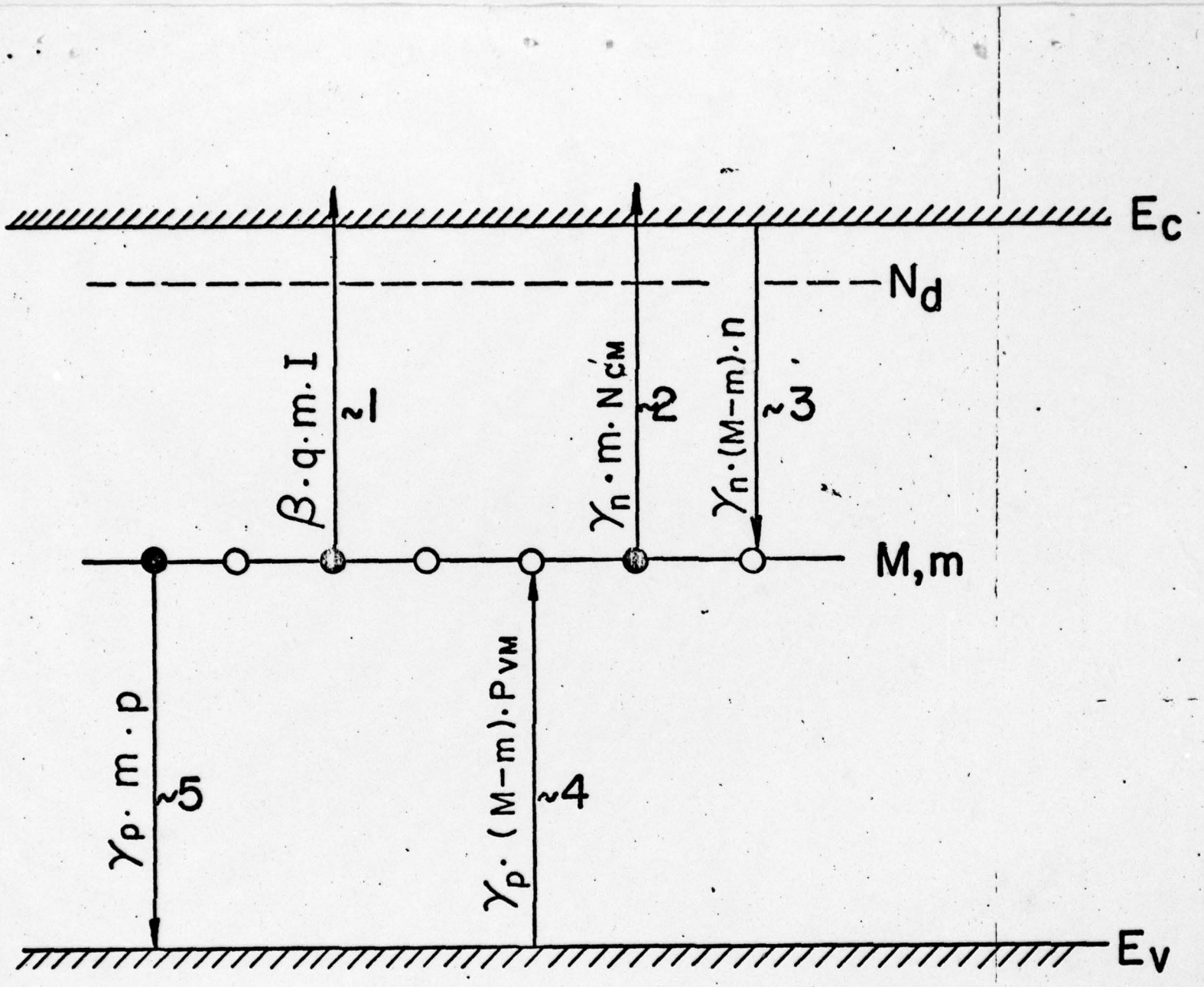


Fig. 1